Regional Environmental Change (2023) 23:92
https://doi.org/10.1007/s10113-023-02084-5

ORIGINAL ARTICLE

Changes in vegetation greenness related to climatic and non-climatic factors in the Sudano-Sahelian region

Yelong Zeng[1,2] · Li Jia[1,3] · Massimo Menenti[1,4] · Min Jiang[1] · Beatrice Asenso Barnieh[1,5] · Ali Bennour[1,2] · Yunzhe Lv[1,2]

Received: 12 November 2022 / Accepted: 27 May 2023 / Published online: 28 June 2023

Abstract

The potential drivers of vegetation changes in the Sudano-Sahelian region of Africa remain poorly understood due to complex interactions between climatic and anthropogenic processes. In this study, we analyzed the vegetation greenness trends in relation to rainfall variability that we considered the essence of climatic effects on vegetation in a well-known water-limited environment by using time series of satellite data in the Sudano-Sahelian region during 2001–2020. We quantified in more detail the relative contributions of rainfall variability (climatic factor), land use/land cover (LULC) change, and fire occurrence change (non-climatic factors) to vegetation greenness trends in selected sub-regions. The results showed that vegetation greening was widespread (26.9% of the total study area), while vegetation browning was more clustered in central West Africa (5% of the total study area). About half of the vegetation greening area can be explained by long-term rainfall variability during 2001–2020, but most of the area characterized by a browning trend was unrelated to rainfall variability. An analysis of the relative importance showed that LULC changes had significant local effects on vegetation greenness and that these changes were characterized by a strong spatial heterogeneity in specific sub-regions. Gains in cropland and natural vegetation related to positive land management were probably the dominant drivers of greening in Senegal and Ethiopia. Also, the combined impacts of rainfall variability and LULC changes contributed to greening trends in the arid zone, particularly in Mali and Sudan. In contrast, vegetation browning in central West Africa appeared to be driven by cropland gain and natural vegetation loss associated with extensive agricultural production activities. Furthermore, we found that repeated fires for agricultural expansion in central West Africa intensified vegetation browning. These results advanced our understanding of vegetation dynamics in response to climatic and non-climatic factors in Sudano-Sahelian drylands characterized by increasing pressures on land resources.

Keywords Vegetation greenness change · NDVI · Relative importance · Rainfall · LULC changes · Fire occurrence

Communicated by Victor Resco de Dios

✉ Li Jia
jiali@aircas.ac.cn

Yelong Zeng
zengyl2018@radi.ac.cn

Massimo Menenti
m.menenti@radi.ac.cn

Min Jiang
jiangmin@aircas.ac.cn

Beatrice Asenso Barnieh
b.a.barnieh@radi.ac.cn

Ali Bennour
alibennour@radi.ac.cn

Yunzhe Lv
lvyunzhe20@mails.ucas.ac.cn

[1] State Key Laboratory of Remote Sensing Sciences, Aerospace Information Research Institute, Chinese Academy of Sciences, Beijing 100101, China

[2] University of Chinese Academy of Sciences, Beijing 100049, China

[3] International Research Center of Big Data for Sustainable Development Goals, Beijing 100094, China

[4] Faculty of Civil Engineering and Geosciences, Delft University of Technology, Stevinweg 1, 2825 CN Delft, The Netherlands

[5] Earth Observation Research and Innovation Centre (EORIC), University of Energy and Natural Resources, P.O. Box 214, Sunyani, Ghana

Introduction

The Sudano-Sahelian region, located in the transition zone between the Sahara Desert and the tropical savanna in Africa, is one of the largest drylands in the world. This water-limited ecosystem sustains the livelihoods of hundreds of millions of people by providing crop production and livestock forage. Changes in the climate and human activities can easily cause ecological stress in the region (Milas 1984; Wang'ati 1996; Leroux et al. 2017; Abel et al. 2021). Since this region experienced severe droughts in the 1970s–1980s, the degradation of vegetation greenness and productivity has posed a serious threat to regional livelihoods, which has caused widespread concerns worldwide (Giannini et al. 2008; Fensholt et al. 2017; Kusserow 2017; Fu et al. 2021). Numerous studies based on in situ and satellite observations suggest that vegetation greenness and productivity in the Sahel have increased with increasing rainfall since the mid-1980s (Herrmann et al. 2005; Hickler et al. 2005; Olsson et al. 2005; Fensholt and Rasmussen 2011; Dardel et al. 2014a, 2014b; Kaptué et al. 2015). In certain areas of the Sudano-Sahelian region, however, a decrease in vegetation greenness, known as browning, has been reported (Leroux et al. 2017; Chen et al. 2019; D'Adamo et al. 2021).

With the booming development of remote sensing technology, a growing number of studies used the satellite-based Normalized Difference Vegetation Index (NDVI), a spectral ratio index based on the red and infrared bands and closely linked to vegetation photosynthetic activity, to investigate changes in vegetation conditions. One of the most important findings has shown that rainfall is the primary driver of vegetation biodiversity and growth in the Sudano-Sahelian region, and thus rainfall is usually considered the essence of climatic drivers (Fensholt and Rasmussen 2011; Fensholt et al. 2017; Kusserow 2017; Zhang et al. 2018, 2019; Brandt et al. 2019). Rainfall determines water availability in arid and semi-arid ecosystems, and in turn, soil water content regulates biomass production by regulating both evapotranspiration and photosynthesis (Noy-Meir 1973; Le Houérou 1984; Fensholt and Rasmussen 2011). Furthermore, the response of vegetation activity in African dryland to rainfall generally lags by 1 month (Li et al. 2019), and has an interannual ecological memory effect (Martiny et al. 2005; Camberlin et al. 2007). Recent research by Zhou et al. (2021a) measured the response of vegetation to rainfall at multiple temporal scales by using the Transfer Function Analysis (TFA) method. These findings were explained to a large extent by the "pulse-reserve" mechanism in the vegetation response to rainfall and significantly enhanced our understanding of environmental change in the Sudano-Sahelian region over the past few decades.

However, multiple studies have demonstrated that rainfall, which is regarded as the primary climatic driver, may not fully explain the vegetation trends recorded by satellite observations (Helldén and Tottrup 2008; Huber et al. 2011; Boschetti et al. 2013; Rasmussen et al. 2014; Hoscilo et al. 2015; Rishmawi and Prince 2016; Leroux et al. 2017). Many non-climatic factors, including land use/land cover (LULC) (Leroux et al. 2017; Brandt et al. 2018), soil properties (Mills et al. 2013), fires (Venter et al. 2018), and wars (Gorsevski et al. 2012), influence vegetation dynamics at various temporal and spatial scales. Among these non-climatic influences, LULC changes have a direct and widespread effect on vegetation dynamics in the Sudano-Sahelian region (Barnieh et al. 2020; Herrmann et al. 2020). LULC changes include all land changes that occur on the Earth's surface, excluding cyclical changes that are often caused by vegetation phenology and snow/ice seasonality, and mainly include conversions and modifications between natural and anthropogenic land cover, agricultural land management, urbanization, overgrazing, and afforestation (Song et al. 2018; Barnieh et al. 2020; Herrmann et al. 2020; D'Adamo et al. 2021; Zhu et al. 2022). Recent studies on vegetation change have emphasized the importance of local LULC changes and their effects (Tappan et al. 2004; Leroux et al. 2014, 2017; Rasmussen et al. 2014; Tong et al. 2017). Therefore, it is necessary to further explore the impacts of multiple interactions between rainfall variability and LULC change on vegetation greenness. However, to determine this, three important issues need to be considered.

First, most studies explored the long-term trends in vegetation greenness and their responses to influence factors using remote sensing vegetation products at a low spatial resolution in the region (Fensholt and Rasmussen 2011; Dardel et al. 2014a; Tian et al. 2016), such as Global Inventory Modelling and Mapping Studies (GIMMS) NDVI product (~ 8 km) and vegetation optical depth (VOD) microwave product (~ 25 km), which cannot capture the spatial heterogeneity of vegetation conditions in fragmented landscapes as usually found in the Sudano-Sahelian region. It is therefore essential to investigate further vegetation greenness trends and drivers by using remote sensing data with higher spatial resolution under ongoing environmental changes in the region for a better understanding of dryland sustainability. Second, LULC products with coarser spatial resolution (e.g., 500 m and 1 km) cannot reflect the fine details of LULC heterogeneity typically found in fragmented landscapes, which hampers a complete understanding of the ecological effects of LULC changes (Zoungrana et al. 2018; Jin et al. 2021; Masiliūnas et al. 2021). In addition, the LULC classification types are usually represented as class numbers, which are not as convenient as continuous values for change analysis, especially when they need to be linked to other variables. The use of land cover fractional abundance derived from higher spatial resolution LULC data to characterize the LULC change may be a possible solution to this problem. Recently, it has been shown that the continuous fractional

LULC approach allows better quantification of ecological response and feedback than categorical LULC (Song et al. 2018; Rigge et al. 2019; Masiliūnas et al. 2021; Borges et al. 2022). Therefore, it is expected that fractional LULC components can better depict the variety of long-term change trajectories and lead to credible attribution of LULC-related changes in vegetation dynamics. Third, fire occurrence, an important non-climatic factor, has a major impact on vegetation greenness and land cover structure of African dryland ecosystems (Archer et al. 2017; Venter et al. 2018; Zubkova et al. 2019; Wei et al. 2020; Ramo et al. 2021). Studies have revealed, however, that variations in rainfall, LULC, and fires in the Sudano-Sahelian region are highly heterogeneous (Pausas and Ribeiro 2013; Herrmann et al. 2020; Wei et al. 2021; Zhou et al. 2021a), and the mechanism by which these elements influence vegetation dynamics remains unclear.

This research aims to investigate the trends in vegetation greenness in the Sudano-Sahelian region over the last 20 years using remote sensing data (i.e., NDVI as a proxy for vegetation condition), as well as the roles of potential drivers. In this study, we considered the dominant climatic effects as rainfall-driven changes, since this is the essence of climatic influence on vegetation dynamics in this region, and the effects of LULC and fires as non-rainfall-driven changes. The specific objectives were to (1) examine the recent vegetation greenness trends in relation to rainfall and (2) explore the relative contributions of rainfall, LULC, and fire occurrence to vegetation greenness trends by using high spatial information in hotspot sub-regions.

Study area and data

Study area

The Sudano-Sahelian region in Africa is an arid and semi-arid belt located between the Sahara Desert and the sub-humid regions north of the equator (Wang'ati 1996; Kusserow 2017). In this paper, we used the aridity index (AI, the ratio of reference evapotranspiration to rainfall) provided by the Consultative Group for International Agriculture Research-Consortium for Spatial Information (CGIAR-CSI) (see Table 1 and the "Other dataset" section) to characterize the study area (Fig. 1). The average annual rainfall in the region increases from less than 100 to more than 1000 mm (Fig. 1b). The western part of the study area is mainly controlled by the West African Monsoon with seasonal rainfall characterized by a rainy season from June to October (Lebel et al. 2009; Nicholson 2009, 2013). The rainfall pattern in East Africa shows a distinct heterogeneity compared with West Africa (Fig. 1b). This is mainly because of the influence of equatorial Pacific and Indian Ocean sea surface temperature (SST) and complex topography (Nicholson 2017; Endris et al. 2019). Such climatic conditions support a wide succession of ecosystems that closely follow the rainfall gradient, such as grassland, savanna, shrubland, dry forests, and humid forests (Bond et al. 2005; Staver 2018; Stevens et al. 2022) (Fig. 1c and d). Land cover in the region is increasingly affected by human imprints due to rapid population growth, mainly characterized by expanding agricultural land and natural vegetation loss (Barnieh et al. 2020, 2022; Herrmann et al. 2020). Although the fire occurrence in Africa decreased during the last two decades, the impact of fires on the vegetation system is rather a complex heterogeneity under the influence of climate change and human activities (Pausas and Ribeiro 2013; Andela et al. 2017; Zubkova et al. 2019; Wei et al. 2020; Ramo et al. 2021).

Data sources and pre-processing

Multiple long-term datasets were used in this study. Details are described in the Table 1 and following sections.

Table 1 Datasets used in the study

Variable	Data source	Spatial resolution	Temporal resolution	Available link
NDVI	MOD13A2 Collection 6	1 km	16-day	https://ladsweb.modaps.eosdis.nasa.gov/archive/allData/6/MOD13A2/
Rainfall	CHIRPS, Version 2.0	0.05° (~5 km)	Monthly	https://data.chc.ucsb.edu/products/CHIRPS-2.0/
Aridity index	CGIAR-CSI	0.0083° (~1 km)	——	https://figshare.com/articles/dataset/Global_Aridity_Index_and_Potential_Evapotranspiration_ET0_Climate_Database_v2/7504448/3
Land use/land cover	Sahel 30	30 m	2000/2005/2010/2015/2020	https://www.tpdc.ac.cn/en/data/1b128d7a-ccf6-4930-99b8-1ec23c8f4160/
Burned area	FireCCI51	250 m	Monthly	https://catalogue.ceda.ac.uk/uuid/58f00d8814064b79a0c49662ad3af537

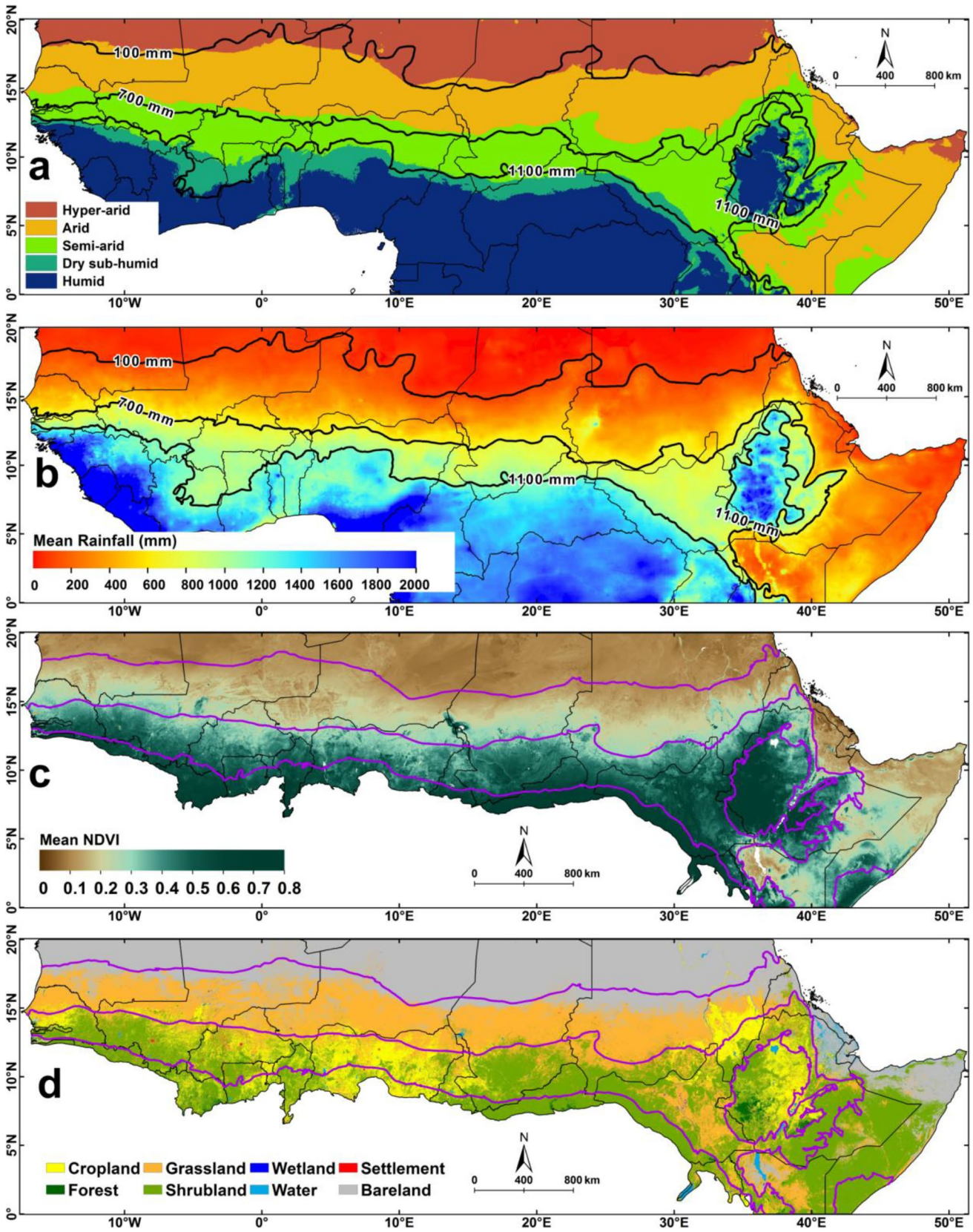

Fig. 1 The study area of Sudano-Sahelian region in Africa: **a** the aridity index (AI) (CGIAR-CSI), **b** mean annual rainfall in 2001–2020 (CHIRPS), **c** mean annual NDVI in 2001–2020 (MOD13A2), and **d** land use/land cover (LULC) map (Sahel 30). The black lines in **a** and **b** represent the rainfall isohyets; the purple lines in **c** and **d** represent the boundaries of aridity regions defined by AI values in **a** (see the "Other dataset" section)

Moderate resolution imagery spectroradiometer normalized difference vegetation index time series data

A 16-day NDVI time series dataset during 2001–2020 at 1 km spatial resolution from the Moderate Resolution Imagery Spectroradiometer (MODIS) products (MOD13A2 Collection 6) was used in this study. The MODIS NDVI is produced using atmospherically corrected surface reflectance and preprocessed with the CV-MVC (Constrained View angle-Maximum Value Composites) algorithm to retain the best quality observations every 16 days. Nonetheless, cloud cover throughout the long rainy season may cause exceptionally low NDVI values, particularly in the southern Sudano-Sahelian region (Leroux et al. 2017). To this end, an improved Harmonic ANalysis of Time Series (iHANTS) algorithm (Zhou et al. 2016, 2021b) was used to reconstruct the NDVI time series, further reducing noise caused by cloud cover. The iHANTS method is an updated tool that improves the original HANTS (Menenti et al. 1993) for time series reconstruction, which applies the Fourier transform theory with several reasonable parameter settings, including inter-annual harmonic components, dynamic fitting error tolerance (FET) scheme, and dynamic update of weights to remove the outliers and fill the gaps in the time series. To eliminate the permanent bare lands and water bodies, the areas with maximum annual NDVI smaller than 0.2 were masked. Later, the reconstructed 16-day NDVI time series were used to calculate the annual mean NDVI for subsequent trend analysis.

Climate hazards group infraRed precipitation with station rainfall data

The monthly rainfall dataset at 0.05° spatial resolution was provided by the Climate Hazards Group InfraRed Precipitation with Station (CHIRPS, Version 2.0), which was produced by combining satellite rainfall estimates, reanalysis climate data, and in situ rain gauge observations (Funk et al. 2015). The CHIRPS data can accurately capture the dynamic changes of rainfall in Africa and are widely used in climate change research and environmental monitoring (Toté et al. 2015; Dembélé and Zwart 2016; Zhou et al. 2021a). The bilinear resampling method was used to resample the monthly CHIRPS rainfall data from 0.05° to 1 km to match the MODIS NDVI data for analysis of the relationship between NDVI and rainfall. We also compared the temporal patterns of rainfall with bilinear resampling resolution and rainfall with original nominal resolution in the similar rainfall belt and north–south rainfall gradient transition zones, and found that the differences between the two datasets could be ignored (Fig. S1).

Land use/land cover dataset

In this study, we used 30 m land use and cover maps for the Sahel-Sudano-Guinean region of Africa (20°W–60°E, 0–25°N) developed by Tsinghua University every 5 years from 1990 to 2020 (namely Sahel 30) (Yu 2022). This dataset uses a collaborative framework of land cover classification based on machine learning and multiple data fusion method to integrate the supervised land cover classification with existing 30 m thematic land cover maps, including Global Forest Change (Hansen et al. 2013), JRC Yearly Water Classification History (Pekel et al. 2016), and annual Global Artificial Impervious Area (Gong et al. 2020) using Google Earth engine (GEE) cloud computing platform. Further details on the methodological approach used to produce this LULC dataset can be found in Xu et al. (2018) and Zhao et al. (2021a). The dataset has been validated using the global validation sample set developed by Li et al. (2017), which includes 19,600 validation samples spanning all the seasons in the Sahel-Sudano-Guinean region. The overall accuracy of the dataset is approximately 75% (Yu 2022). Sahel 30 provides eight LULC classes, i.e., cropland, forest, grassland, shrubland, wetland, water, impervious surface (settlement), and bareland. The eight LULC classes from 2000 to 2020 were aggregated into cropland, natural vegetation (forest, grassland, and shrubland), and non-vegetation (wetland, water, settlement, and bareland). To analyze the heterogeneity of LULC changes at lower spatial resolution (1 km) for a better linkage with the NDVI observations, the fractional abundance of each class within each 1 km pixel was calculated using the LULC Sahel 30 data.

Burned area product

The burned area (BA) product in 2001–2020 was provided by the monthly fire information at 250 m resolution from the Climate Change Initiative (CCI) project of the European Space Agency (ESA), namely FireCCI51. This BA product is generated from the MODIS daily surface reflectance data product (MOD09GQ) at 250 m spatial resolution and the MODIS global monthly fire location product (MCD14ML) with active fire information based on thermal bands. The algorithm detects burned pixels by applying the contextual region growing method to the fire seed, which introduces adaptive cluster threshold filtering (Lizundia-Loiola et al. 2020). Compared with other global burned area products, FireCCI51 improves the detection of small fires, which is very important for correctly estimating the actual burned area, especially in areas with widespread agricultural activities, such as in the Sudano-Sahelian region (Lizundia-Loiola et al. 2020; Ramo et al. 2021). The validation based on sampled sites of FireCCI51 shows that the omission and commission errors of Africa, i.e., 54.5% and 25.7%, are lower than the global ones, i.e., 67.1% and 54.4% (Lizundia-Loiola et al. 2020). The annual sum of monthly burned area within a 1 km pixel was used as an index of fire occurrence and intensity.

Other dataset

The aridity index (AI) data developed by the Consultative Group for International Agriculture Research-Consortium for Spatial Information (CGIAR-CSI) (Trabucco and Zomer 2018) were used to define the boundary of the Sudano-Sahelian region in this study, including the hyper-arid ($AI \leq 0.03$), arid ($0.03 < AI \leq 0.2$), semi-arid ($0.2 < AI \leq 0.5$), dry sub-humid ($0.5 < AI \leq 0.65$), and the humid zone of the East African Plateau ($AI > 0.65$).

Methods

In this study, the trend of vegetation greenness in the Sudano-Sahelian region between 2001 and 2020 was estimated using MODIS NDVI time series data. Then, the impacts of rainfall, LULC, and fire occurrence on the trends in vegetation greenness at the pixel and sub-region level were assessed using statistical attribution methods, i.e., the correlation-based conceptual attribution model and relative importance approach (Fig. 2).

Trend analysis

The Thiel-Sen and Mann–Kendall (MK) test are common methods for estimating long-term trends in environmental variables (Ahmedou et al. 2008; Chen et al. 2019). The Thiel-Sen method was used to estimate the trends in NDVI, rainfall, LULC fraction, and burned area. The Yue-Pilon pre-whitening MK test (Yue et al. 2002) was used to assess the significance of the trends at the 95% level ($p < 0.05$). A significant positive slope of NDVI indicates vegetation greening, and a significant negative slope indicates vegetation browning.

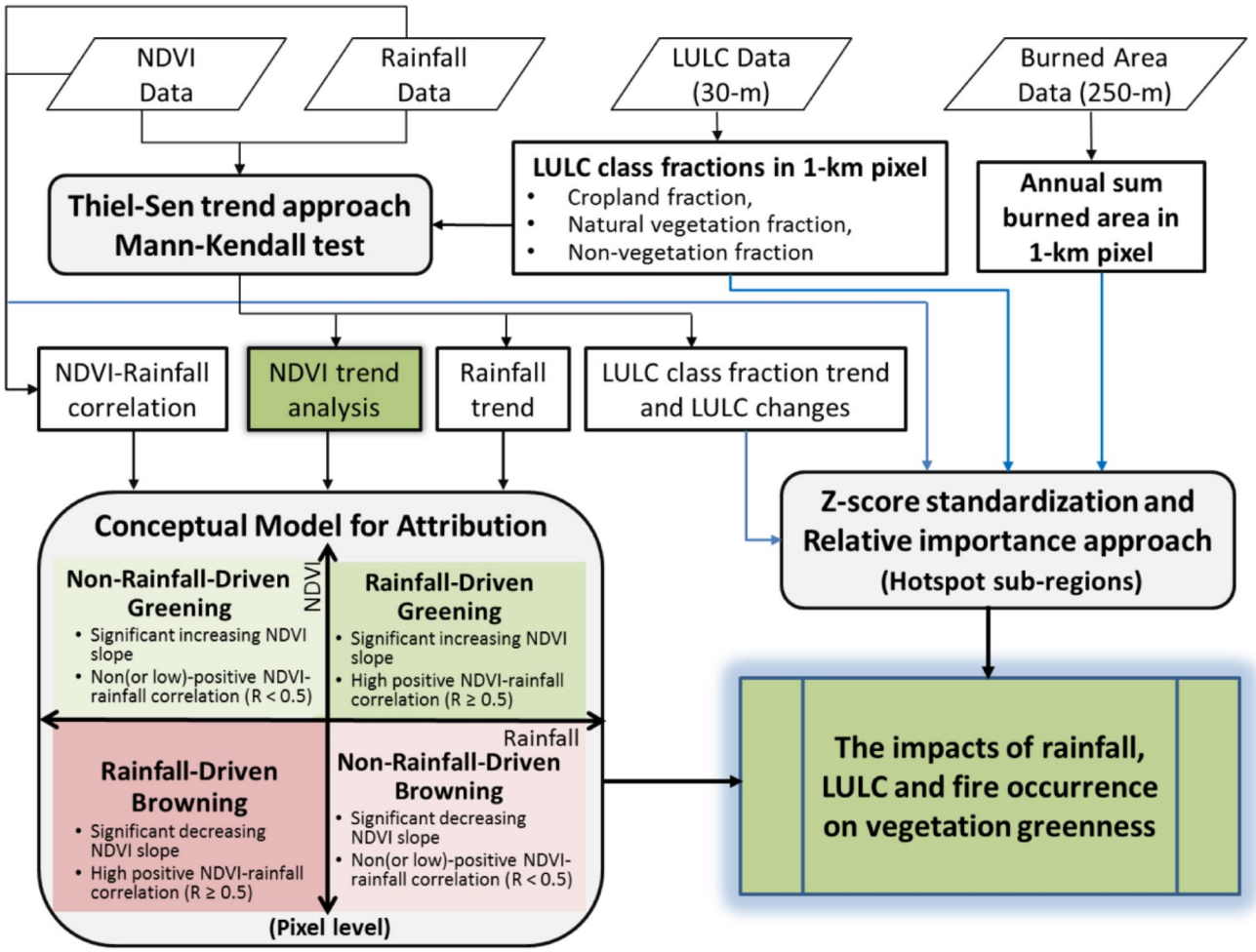

Fig. 2 Flowchart of the study. Correlation-based conceptual attribution model was used to examine the recent NDVI trends in relation to rainfall at pixel level. The relative importance approach was used to explore the relative contributions of rainfall, LULC, and fire occurrence to NDVI trends in hotspot sub-regions

Determining drivers of vegetation greenness trends

Attribution of greenness changes to rainfall

A conceptual model for attribution based on Pearson's correlation analysis was applied to understand how much of the observed trends in vegetation greenness could be explained by rainfall at the pixel level (Hoscilo et al. 2015; D'Adamo et al. 2021). To evaluate the response of vegetation to rainfall at different time scales, three different annual rainfall composites were built by accumulating monthly rainfall from (a) previous year (1-year lag), (b) December of previous year to November of current year (1-month lag), and (c) current year (zero lag). The pixel-wise Pearson correlation (R) between annual mean NDVI and annual accumulated rainfall (with and without time-lag) was then calculated. Subsequently, pixel-wise significant trends in annual mean NDVI, significant trends in annual rainfall, and strong positive NDVI-rainfall correlation with and without time-lag ($R \geq 0.5$) were extracted to assess the driver of rainfall on vegetation greenness changes. Those pixels where both annual mean NDVI and annual rainfall with and without time-lag increased (decreased) in 2001–2020 were identified as rainfall-driven greening (browning), while the remaining pixels were identified as non-rainfall-driven greening (browning) and will be further analyzed.

Attribution of potential drivers in the sub-regions

To assess the influence of potential drivers on NDVI trends identified as rainfall-driven/non-rainfall-driven greening (browning), the contributions of rainfall, LULC fraction, and fire occurrence were estimated using a Z-score standardization and the Lindeman-Merenda-Gold (LMG) approach. First, the NDVI and potential drivers, i.e., rainfall, burned area, fractional abundance of cropland, natural vegetation, and non-vegetation in each year, were standardized using the pixel-wise Z-score method (Eq. 1), which is an effective method for converting different scales to the same comparable scale so that anomalies in different variables are comparable (Helldén and Tottrup 2008; D'Adamo et al. 2021):

$$Z = \frac{x - \mu}{\sigma} \tag{1}$$

where x is the annual value of a variable in each pixel (grid); μ and σ are the mean and standard deviation of variable x over 2001–2020, respectively.

We then calculated the spatial averages of the Z-score values of annual NDVI (Z_{NDVI}), rainfall (Z_{Rf}), cropland fraction (Z_{Cr_f}), natural vegetation fraction (Z_{NatV_f}), non-vegetation fraction (Z_{NonV_f}), and burned area (Z_{BA}), and applied them to the LMG approach (Eq. 2).The LMG algorithm estimates the relative importance of each variable by decomposing the sum of squares (R^2) into non-negative contributions shared by each variable for multiple linear regression models (Lindeman et al. 1980), expressed as the Pearson correlation in a multiple linear regression:

$$\begin{aligned} Z_{NDVI} = {} & a_0 + a_1 \times Z_{Rf} + a_2 \times Z_{Cr\_f} + a_3 \times Z_{NatV\_f} \\ & + a_4 \times Z_{NonV\_f} + a_5 \times Z_{BA} + \varepsilon \end{aligned} \tag{2}$$

where ε denotes other drivers that were not considered but might contribute to NDVI variation. The LMG relative importance values were obtained by averaging the sequential sum of squares (R^2) for all possible orders, and all relative importance values were normalized (divided by R^2) to sum to 1. The algorithm was applied using the "relaimpo" package in R (Grömping 2006).

To further assess the impact of LULC change on NDVI, the violin plots and the Mood median test (Mood 1950) were used to compare the differences in the frequency distributions of NDVI pixel values under the LULC changes in the periods 2001–2010 and 2011–2020 in the sub-regions. Furthermore, the historical Google Earth images with high spatial resolution (~2 m) were used to confirm LULC changes by visual comparison in different years for the sub-regional analysis. In this paper, the LULC change was defined as the change in the fractions of the three LULC classes (cropland, natural vegetation, and non-vegetation) in each 1 km LULC pixel, and the total change over 2000–2020 was calculated by multiplying the slope of the Thiel-Sen trend of LULC change (i.e., the change in fraction of each one of the three classes) by 20 years. If the trends of the fractions of the three LULC classes in a pixel from 2000 to 2020 were zero, then "no change" in LULC was defined, and the class with the maximum fraction was assigned as the main LULC class of that pixel; otherwise, we defined a paired LULC change according to the maximum gain (maximum positive trend value) and the maximum loss (minimum negative trend value). Thus, six paired LULC change types were defined: (1) cropland gain with natural vegetation loss (i.e., Cr↑-NatV↓); (2) cropland gain with non-vegetation loss (i.e., Cr↑-NonV↓); (3) natural vegetation gain with cropland loss (i.e., NatV↑-Cr↓); (4) natural vegetation gain with non-vegetation loss (i.e., NatV↑-NonV↓); (5) non-vegetation gain with cropland loss (i.e., NonV↑-Cr↓); (6) non-vegetation gain with natural vegetation loss (i.e., NonV↑-NatV↓) (Fig. S2).

Results

Trends in vegetation greenness

The results showed that 32.1% of the Sudano-Sahelian region were characterized by significant NDVI trends ($p < 0.05$) during 2001–2020, while in the remaining 67.9%

of the NDVI trends were not significant (Fig. 3a). Within the areas with significant pixel-wise trends in NDVI, 84% were positive, indicating greening. Specifically, greening trends were observed in the Sahel arid zone, western semi-arid zone of West Africa (west of Burkina Faso and Côte d'Ivoire), Sudanian savannah (eastern Chad, Sudan, and South Sudan), and Ethiopia, with the most pronounced greening in Mali and South Sudan.

The extent of browning (significant negative NDVI trends) in 2001–2020 was much smaller, accounting for 5.3% of the Sudano-Sahelian region only. The browning trends were observed in the semi-arid zone and dry subhumid zone of West Africa (Benin, Niger, Nigeria, and southern Chad), Kenya, and Somalia (Fig. 3a).

We evaluated the contributions of the LULC change types to greening or browning trends along with the aridity index gradient in the entire Sudano-Sahelian region (Fig. 4). In arid and semi-arid zones (under drier conditions, i.e., AI ≤ 0.65), the greening trends (Fig. 4a) occurred mostly in areas covered by natural vegetation, whereas in the humid zones of the East African Plateau, they distributed more in agricultural land (cropland and cropland gain). As regards the browning trends (Fig. 4b), they mainly occurred in agricultural land (cropland and cropland gain) with a steep increase from the semi-arid zone through the humid zone. Overall, significant vegetation trends mainly distributed in natural vegetation, and they were also distributed in areas associated with LULC changes, especially the human-induced agriculture lands, increasing from the arid to humid zone.

Correlation between vegetation greenness trend and rainfall variability

The response of NDVI to rainfall in the Sudano-Sahelian region was evaluated by the Pearson correlation coefficient (Fig. 5). The correlation coefficient between annual mean NDVI and total annual rainfall in 2001–2020 showed that 35% of the study area were characterized by strong positive correlations ($R \geq 0.5$), mainly along the Sahel belt, eastern South Sudan, northern Uganda, and arid areas of East Africa (Ethiopia, Kenya, and Somalia) (Fig. 5a). The Pearson correlation coefficients at 1-year lag (marked as $R_{lag\text{-}y}$), 1-month lag (marked as $R_{lag\text{-}m}$), and zero lag (marked as $R_{lag\text{-}0}$) were displayed as a RGB color composite as shown in Fig. 5b. In general, the spatial patterns of NDVI-rainfall correlation at 1-month lag and correlation zero lag were very similar.

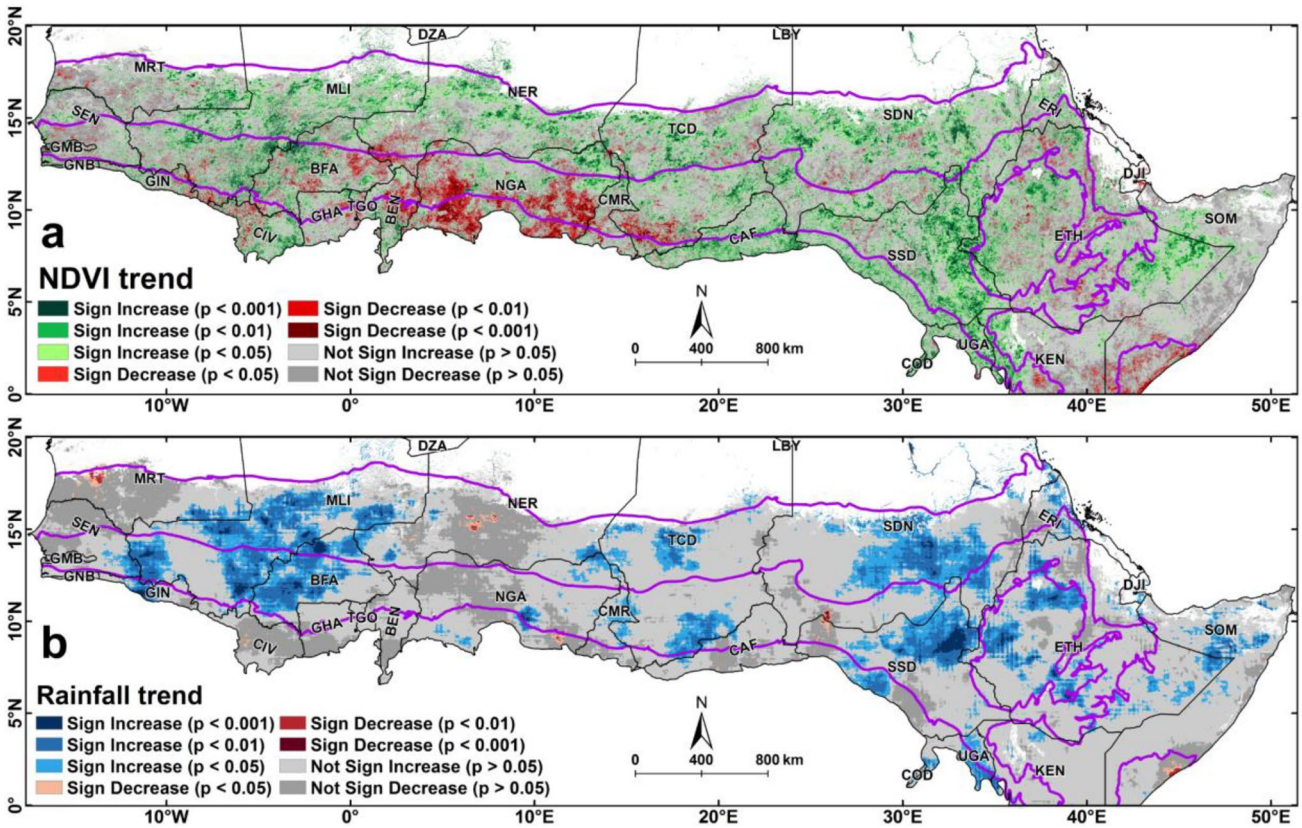

Fig. 3 Map of trends in **a** annual mean NDVI and **b** annual rainfall over the Sudano-Sahelian region in 2001–2020. Gray areas show insignificant trends ($p \geq 0.05$). Pixels with very low NDVI (annual maximum NDVI < 0.2) are masked. The results show that the vegetation greening in West Africa and Sudanian savannah spatially overlapped with areas of increased annual rainfall

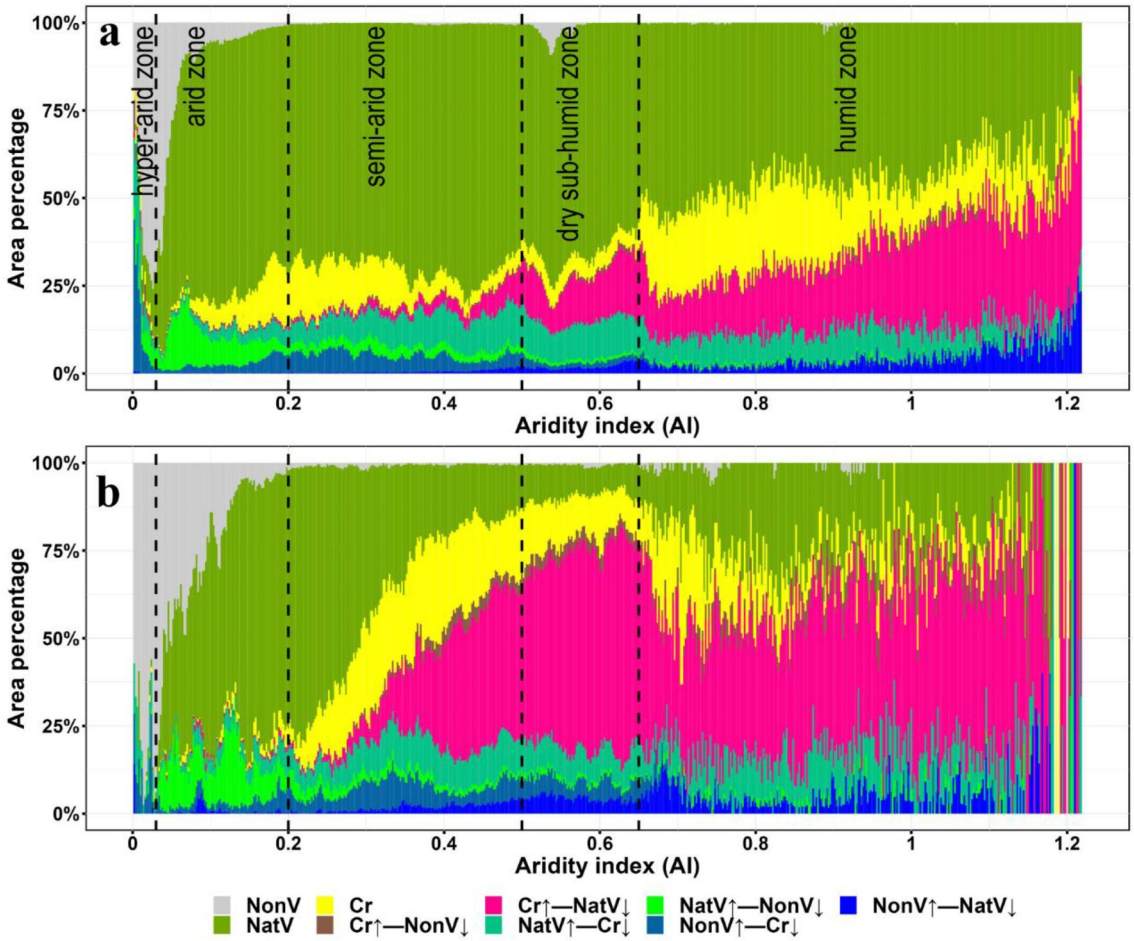

Fig. 4 Fractional abundance of LULC change types contributing to **a** greening and **b** browning vs. aridity index (AI); the bin width of AI values (*x*-axis) was set to 0.002. The vertical dashed lines indicate the climate zones divisions used in this paper. For the meaning of the legends, refer to the definition of LULC change given in the "Attribution of potential drivers in the sub-regions" section (single class without the arrow indicates no change over 2001–2020)

However, a relatively clustered positive correlation between annual mean NDVI and the previous year's rainfall (i.e., $R_{lag\text{-}y}$) (corresponding to the red areas in Fig. 5b) was found in areas where the response of NDVI to concurrent rainfall was not significant as seen in Fig. 5a, mainly in the hyper-arid zones (e.g., northern Mauritania and Somalia) and the semi-arid zone (e.g., southern Senegal, southern Mali, and southern Sudan). The clustered positive correlation between annual mean NDVI and the previous year's rainfall indicated that this correlation coefficient ($R_{lag\text{-}y}$) was much larger than both $R_{lag\text{-}m}$ and $R_{lag\text{-}0}$ at these locations.

Approximately 49% (about 968,974 km^2) of the total greening area showed an increase in vegetation greenness that could be explained by rainfall, i.e., rainfall-driven greening (Fig. 5c). This occurred mainly in arid and semi-arid areas with significant increases in rainfall during 2001–2020 (Fig. 3b), such as Mali, western Burkina Faso, Chad, Sudan, South Sudan, and northern Uganda. In contrast, non-rainfall-driven greening appeared mainly in Senegal, Niger, Central Africa, western South Sudan, and northern Ethiopia, accounting for 51% of the total greening area (about 1,005,587 km^2).

The extent of rainfall-driven browning was small and scattered, accounting for 4% of the total browning area (about 17,140 km^2). Non-rainfall-driven browning was clustered in Benin, southern Niger, Nigeria, and southern Chad, accounting for 94% of the total browning area (about 368,924 km^2).

Importance of potential drivers in the sub-regions

In addition to identifying rainfall-driven changes in vegetation greenness, we conducted potential driver analyses in specific areas to link NDVI trends to rainfall, LULC, and fire occurrence in more detail. The areas with non-rainfall-driven greening (browning), i.e., significant increasing

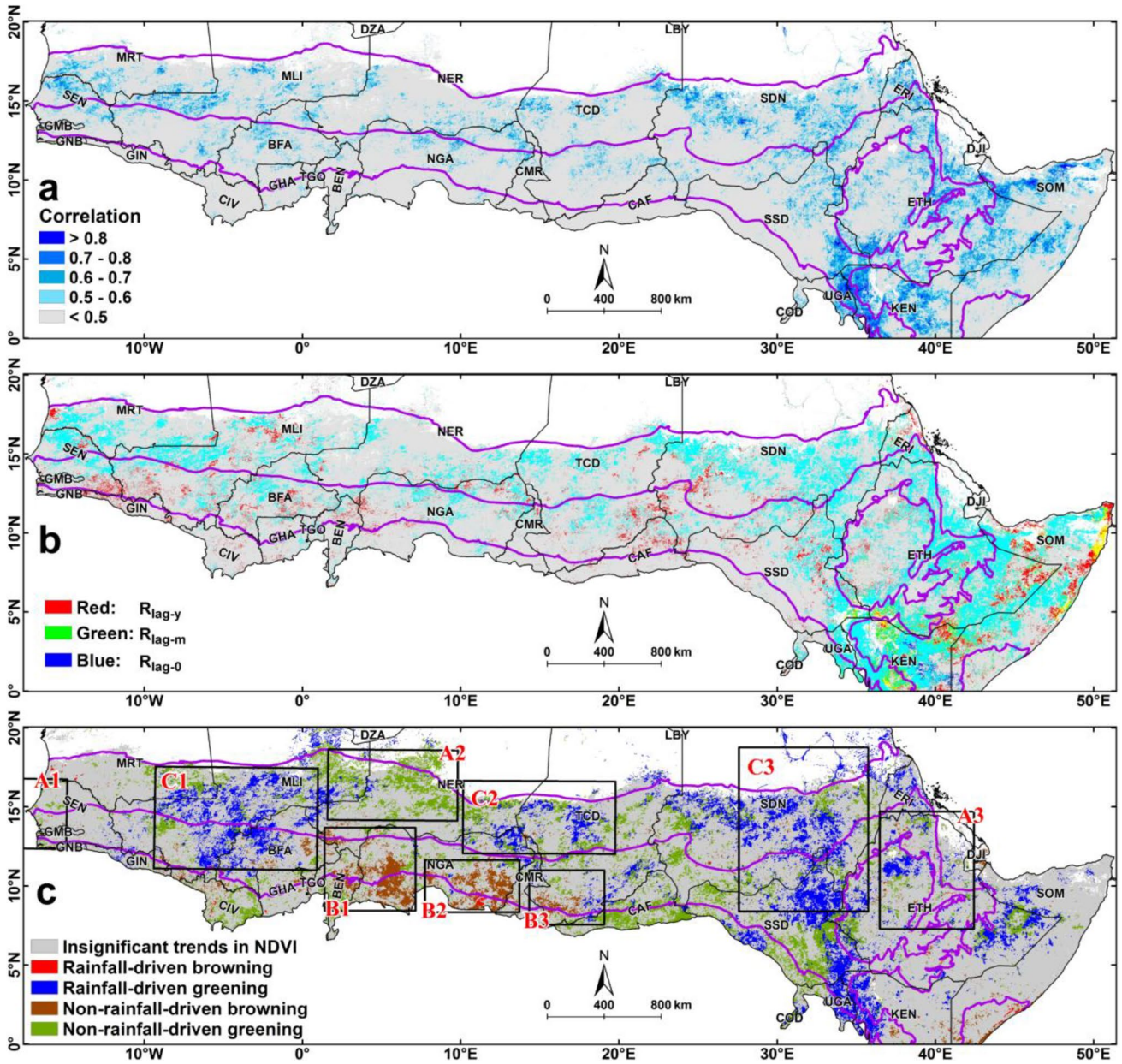

Fig. 5 NDVI response to rainfall in the Sudano-Sahelian region for 2001–2020. **a** Correlation coefficient between annual mean NDVI and annual rainfall in the 2001–2020; **b** the RGB composite of NDVI-rainfall correlation coefficient at different time-lags (Red = $R_{lag\text{-}y}$, Green = $R_{lag\text{-}m}$, and Blue = $R_{lag\text{-}0}$); **c** rainfall-driven and non-rainfall-driven attributions of NDVI trends. $R_{lag\text{-}y}$, $R_{lag\text{-}m}$, and $R_{lag\text{-}0}$ represent 1-year lag, 1-month lag, and zero lag in the response of NDVI to rainfall, respectively. The gray areas in **a** and **b** show low correlation coefficients ($R < 0.5$). The cyan color in **b** represents a strong positive NDVI-rainfall correlation ($R \geq 0.5$) in both $R_{lag\text{-}m}$ and $R_{lag\text{-}0}$, while yellow represents strong positive NDVI-rainfall correlation in both $R_{lag\text{-}y}$ and $R_{lag\text{-}m}$. The black boxes in **c** are the nine hotspot sub-regions selected to analyze the impacts of potential drivers on vegetation greenness trends, including non-rainfall-driven greening clusters, i.e., A1: Senegal, A2: central Niger, and A3: Ethiopia; non-rainfall-driven browning clusters, i.e., B1: Benin-Niger-Nigeria, B2: eastern Nigeria, and B3: southern Chad; and rainfall-driven greening clusters, i.e., C1: western Sahel (Mali and western Burkina Faso), C2: western Chad, and C3: Sudanian savannah (Sudan and South Sudan)

(decreasing) NDVI slope but negative or low positive NDVI-rainfall correlation ($R < 0.5$), and areas with rainfall-driven greening, i.e., significant increasing NDVI slope and high positive NDVI-rainfall correlation ($R \geq 0.5$), were selected as hotspot sub-regions. Analysis of rainfall-driven browning hotspots was excluded due to the very small extent. The sub-regions were labeled in Fig. 5c.

For the non-rainfall-driven greening clusters (Senegal, central Niger, and Ethiopia), the relative importance of rainfall variation, change in fractions of LULC types, and change

in burned area on the NDVI anomalies (i.e., the *Z*-score of NDVI) during 2001–2020 is shown in Fig. 6a–c. The multiple linear regression model (see Eq. 2) showed that the five factors can explain 86.6% of the NDVI anomalies (71% for Senegal, 94% for central Niger, and 95% for Ethiopia, respectively) on average. In general, change in cropland fraction and change in natural vegetation fraction contributed more than rainfall variation in these sub-regions. The total importance of these two LULC types accounted for about 54% of the total importance of all five factors. The factors with the highest importance varied across the regions. In Senegal, the change in cropland fraction was probably the dominant factor contributing to the greening, while the change in natural vegetation fraction was probably the most important factor in central Niger and Ethiopia. The change in burned area factor had weak influences on NDVI anomalies in all non-rainfall-driven greening sub-regions except Senegal.

As shown in Fig. 6d–f, the median values of NDVI with cropland gain (Cr↑-NatV↓) and natural vegetation gain (NatV↑-NonV↓ and NatV↑-Cr↓) exhibited significant differences. It further illustrated that LULC changes played significantly important roles in the greening of these areas. Also, we observed that the NDVI increase in Senegal was associated with non-vegetation gain.

For the non-rainfall-driven browning sub-regions (Benin-Niger-Nigeria, eastern Nigeria, and southern Chad), the relative importance results were somewhat different (Fig. 7a–c). The explanatory of the model in these clusters reached higher determination coefficients (90% for Benin-Niger-Nigeria, 94% for eastern Nigeria, and 90% for southern Chad, respectively). In addition to the change in cropland fraction and change in natural vegetation fraction—the two with the highest relative importance—change in burned area also had a high contribution (ranked third) to the browning of these areas. The total importance of these three factors accounted for more than 90% of all five factors. In contrast, rainfall variation had the lowest influence on NDVI anomalies in all non-rainfall-driven browning sub-regions, even though rainfall was increased (Fig. S4d–f). In terms of NDVI distribution with different LULC changes, cropland gain (Cr↑-NatV↓ and Cr↑-NonV↓) significantly contributed to the browning of these areas (Fig. 7d–f). In addition, a decreased NDVI was observed related to natural vegetation gain with cropland loss. This may be due to cropland had a higher greenness than natural vegetation (mainly grassland and shrubland) and thus had a lower NDVI.

The combined impacts of rainfall variation and LULC change on greening were obvious in the western Sahel, western Chad, and Sudanian savannah (Fig. 8). From the multiple linear regression (Eq. 2) with high determination coefficient (reached 90% on average), the combination of rainfall variation, change in cropland fraction, and change in natural vegetation fraction had the highest relative importance in driving the greening (Fig. 8a–c). The total importance of these three factors accounted for more than 72% of all five factors. In terms of NDVI distribution with different LULC changes, natural vegetation gain (NatV↑- NonV↓) significantly contributed to the greening of these areas (Fig. 8d–f). Also, we observed that non-vegetation gain with natural vegetation loss had a positive influence on greening in western Sahel.

Discussion

Vegetation greenness trends

In this study, we provided a pixel-wise assessment of trends in vegetation greenness in the Sudano-Sahelian region. Based on our analysis using MODIS collection 6 NDVI data (MOD13A2), we found a widespread greening trend during 2001–2020, which is consistent with the trends evaluated in previous studies using different datasets in different time periods, such as SPOT-VGT NDVI (2001–2010) (Hoscilo et al. 2015), MODIS EVI (2001–2009) (Cho et al. 2015), and MODIS NDVI (2000–2015) (Leroux et al. 2017). Our results support the fact that greening is occurring in the Sudano-Sahelian region, which is also corroborated by other greening trends found in global scale studies (Chen et al. 2019; Piao et al. 2020). At the same time, we also found a browning trend clustered in central West Africa. Specifically, Nigeria and southern Niger in central West Africa have been continuously browning since the late twentieth century, as observed using different remote sensing data and applying different analysis techniques (Fensholt and Rasmussen 2011; Dardel et al. 2014a; Cho et al. 2015; Hoscilo et al. 2015; Ahmed et al. 2017; Leroux et al. 2017; Chen et al. 2019; Piao et al. 2020; Ogutu et al. 2021).

Drivers of vegetation greenness changes

Few previous studies focused on the relative contributions of rainfall variability and LULC changes to vegetation greenness trends in the Sudano-Sahelian region, while rainfall factor is the primary concern of such studies (Fensholt and Rasmussen 2011; Fensholt et al. 2017; Zhang et al. 2018, 2019; Brandt et al. 2019; Ogutu et al. 2021; Zhou et al. 2021a). In this study, we analyzed the NDVI trends related to rainfall variability and improved the current understanding of the relative contributions of rainfall variability, LULC change, and fire occurrence change to NDVI trends in specific sub-regions.

Greenness change driven by rainfall variability

Our results found that about half of the area of vegetation greening can be explained by rainfall variability, i.e.,

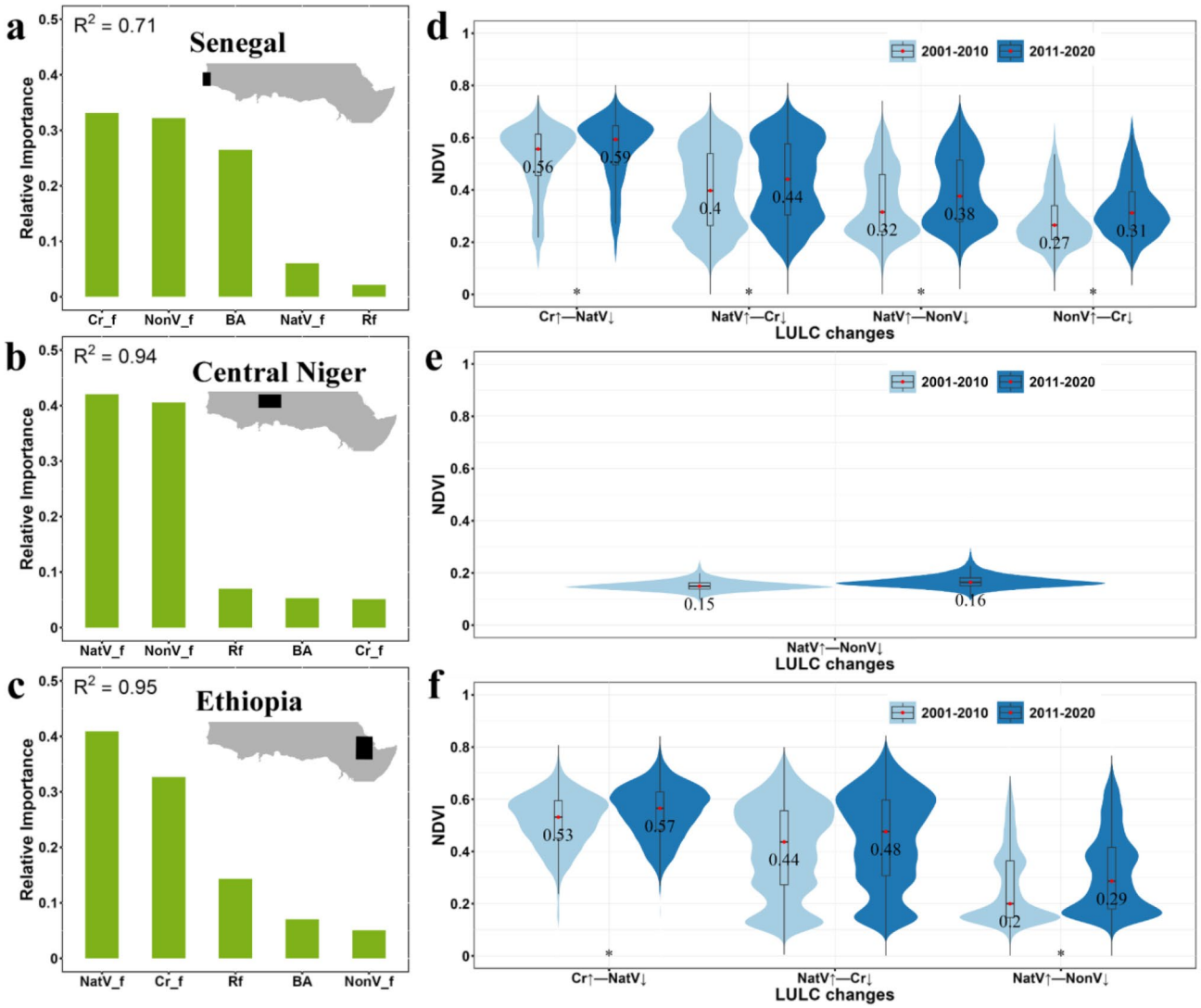

Fig. 6 **a–c** The relative importance of rainfall variation (Rf), change in cropland fraction (Cr_f), change in natural vegetation fraction (NatV_f), change in non-vegetation fraction (NonV_f), and change in burned area (BA) to the NDVI anomalies (*Z*-score of NDVI) within non-rainfall-driven greening clusters in the Sudano-Sahelian region during 2001–2020. R^2 in the figures is the coefficient of determination of the multiple linear regression between the *Z*-score of NDVI and the *Z*-scores of the five factors. **d–f** Corresponding violin diagrams of the NDVI distribution associated with the observed LULC changes in 2001–2010 and 2011–2020. The LULC change types with a low cumulative area percentage in the non-rainfall-driven greening clusters (< 3%) are not shown in the violin diagrams. The red dots and numbers represent the medians of the NDVI values. Violin diagrams with "*" in two periods are different at $p < 0.05$ based on the Mood median test

rainfall-driven greening. Indeed, the greening trends in these areas were related to the increased rainfall due to the northward movement of the West African Monsoon system, as documented by regional climate modelling and remote sensing rainfall data (Ramel et al. 2006; Cook and Vizy 2019). This confirms that water supply is a key limiting factor of the growth of dryland vegetation (Fensholt and Rasmussen 2011; Fensholt et al. 2017; Kusserow 2017; Brandt et al. 2019; Zhang et al. 2019; Jiang et al. 2022). Our results also showed that the influence of previous year's rainfall was larger than the current year's rainfall in the hyper-arid and semi-arid zone. According to the "pulse-reserve" paradigm and similar studies (Noy-Meir 1973; Martiny et al. 2005; Camberlin et al. 2007; Zhou et al. 2021a), rainfall in dryland ecosystems may accumulate at different soil depths with different durations, creating a certain degree of multi-scale soil "memory effect" and then regulate biological processes such as plant growth or reproduction at multiple

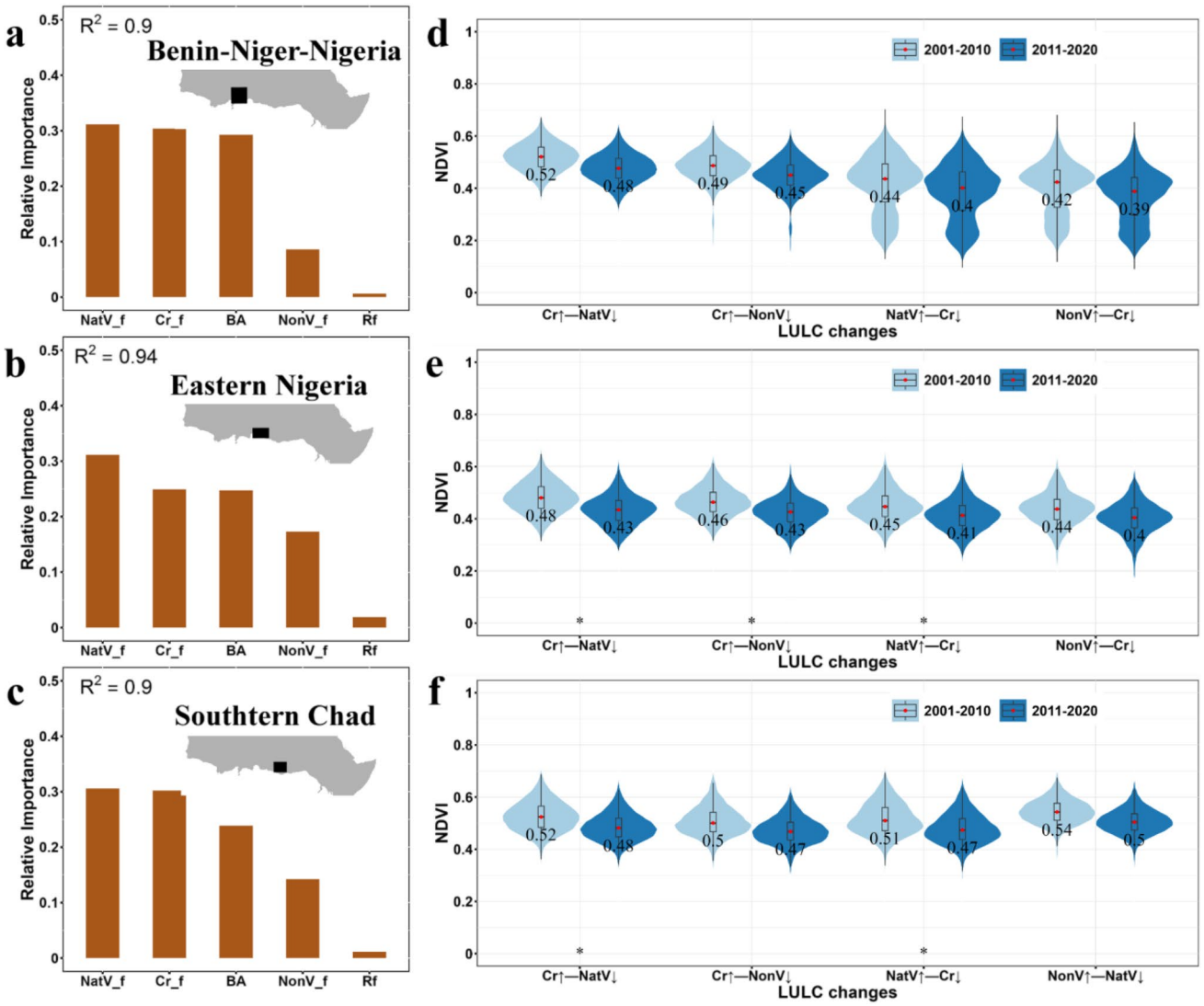

Fig. 7 Same as Fig. 6 but within non-rainfall-driven browning clusters

spatial and temporal scales. In addition, the seasonal distribution of rainfall may also influence vegetation greenness and productivity in the Sudano-Sahelian region (Zhang et al. 2018; Zhou et al. 2021a). For example, an increase in heavy rainfall events, a delayed onset of the rainy season, and dry spells longer than 14 days would result in a considerable decrease in herbaceous vegetation production in the Sahel region (Zhang et al. 2018). In more humid areas, the vegetation greenness is relatively insensitive to rainfall variability because plant growth is limited by other resources (e.g., light and nutrients), rather than water availability (Zhu et al. 2016; Piao et al. 2020). As for other climatic factors, such as temperature and evapotranspiration, they interact to complicate the attribution of changes in vegetation conditions in this water-limited region. On the one hand, global warming will increase evaporative demand and further deplete soil moisture in semi-arid areas, increasing the risk of drought stress in vegetation (Cheng and Huang 2016; Berg and Sheffield 2018). On the other hand, the negative effects of increased evapotranspiration and drought stress under warmer temperatures may be mitigated by wetter climates and by enhanced water use efficiency induced by elevated CO_2 concentrations (Lu et al. 2016; Devine et al. 2017).

Greenness change related to non-climatic factors

In addition to rainfall variability, LULC change is another dominant driver of vegetation greenness changes and varies across regions. LULC changes had considerable local effects on vegetation greenness and exhibited a strong spatial heterogeneity in certain sub-regions of the Sudano-Sahelian region, although the overall effect

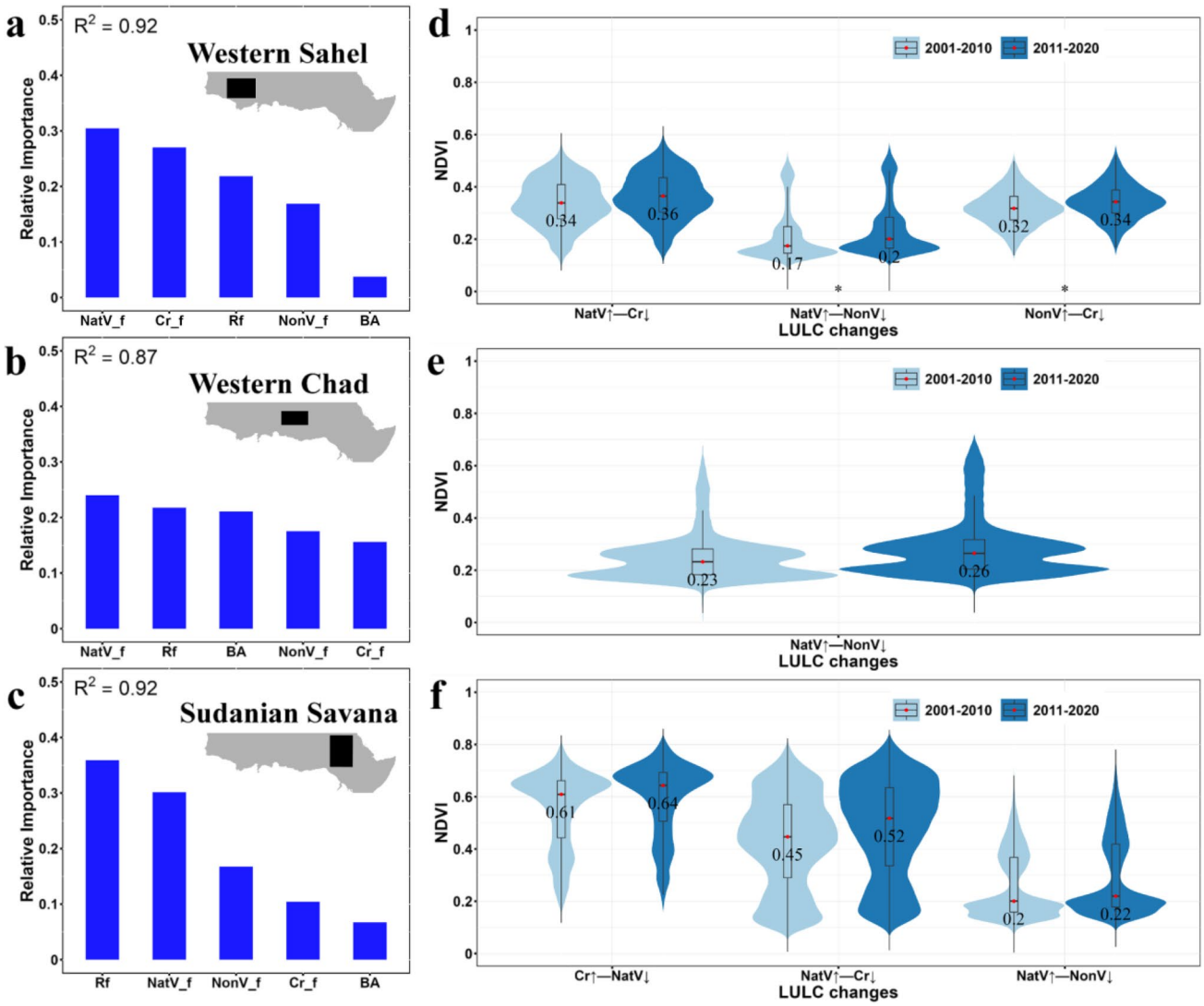

Fig. 8 Same as Fig. 6 but within rainfall-driven greening clusters

of LULC changes on vegetation greening or browning was relatively limited on average across the entire region. We conducted the analysis of LULC change using higher spatial resolution data, which allowed us to quantitatively link the changes in LULC type fractions to changes in vegetation conditions represented by NDVI. Our results suggested that the likelihood of significant vegetation trends in response to LULC changes increased from the arid to the humid zone (Figs. 3 and 4 and Fig. S2), especially with respects to the human-induced agricultural changes, that can be attributed to the expansion of growing human activities due to the increased population density in climatic conditions more suitable for agriculture. Specifically, cropland gain and natural vegetation gain related to land management were probably the two main drivers of the greening in certain sub-regions.

Cropland gain related to agricultural intensification and expansion contributed to a large extent to vegetation greening. Agricultural intensification is usually defined as the process of increasing the agricultural productivity of existing cultivated cropland (Foley et al. 2011; Hu et al. 2020). In this way, farmers use various agricultural management practices such as irrigation, fertilizers, pesticides, mechanization, and improved crop seeds to increase crop productivity (Brandt et al. 2014; Tadele 2017; Oates et al. 2020; Wortmann and Stewart 2021). Furthermore, the greenness after agricultural expansion is higher than that of natural vegetation or semi-natural vegetation, such as savanna and short-grass vegetation in Senegal and Sudan (Ruelland et al. 2010; Bégué et al. 2011; Nutini et al. 2013).

Natural vegetation gain and cropland gain may tentatively be related to the implementation of land restoration projects

and positive natural resource management, which would then contribute to vegetation greening. The Farmer-Managed Natural Regeneration (FMNR) project, a well-known land restoration project, is a widespread practice in the Sahel region of West Africa (Shono et al. 2007; Reij et al. 2009; Brandt et al. 2014). This project encourages local farmers to reforest their agricultural land, focusing on protecting and promoting the regeneration of trees with small and medium size and shrubs in the fields. The implementation of the FMNR project has improved soil fertility and significantly increased tree cover by reducing the frequency of deliberate fires in the croplands in the northern Peanut Basin of Senegal (Camara et al. 2021) (Fig. S5a) and Seno plain of Mali (Pasiecznik and Reij 2020) (Fig. S5b). As of 2010, an estimated 450,000 hectares of land in the Seno Plain of Mali was affected by FMNR (Pasiecznik and Reij 2020). The reforestation rate in this area could reach at least 250 trees per hectare, providing both good ecological and economic value (Pasiecznik and Reij 2020; Kelly et al. 2021). Furthermore, the Enabered watershed in the Tigray region of Ethiopia (Fig. S5c) showed the imprint of the implementation of a series of integrated watershed management projects that favor land restoration (Haregeweyn et al. 2012; Teka et al. 2020). A series of positive measures, such as the constructions of exclosure areas, vegetative hedgerows, drainage channels on cultivated lands and small-scale irrigation systems, and reclamation of degraded wastelands have mitigated the problem of soil erosion caused by the pressure of human activities and effectively increased the vegetation cover in the Enabered watershed, Tigray region (Haregeweyn et al. 2012; Gashaw 2015). Notably, the NDVI increase in certain area of West Africa was associated with non-vegetation gain. This was probably related to the increase of wetland and flooded vegetation affected by seasonal water bodies, such as in southern Senegal (Fent et al. 2019; Andrieu et al. 2020; Ogilvie et al. 2020) and the Inner Niger Delta of Mali (Bergé Nguyen and Crétaux 2015; Kelly et al. 2021).

In contrast, cropland gain with natural vegetation loss associated with extensive agricultural production activities would be the dominant driver of vegetation browning in central West Africa. In these areas, cultivation and grazing are the main livelihood activities due to the most suitable climatic conditions for agriculture, which would lead to the widespread conversion of grassland, shrubs, and forests into cropland and pastures. Our results showed a significant decrease in NDVI (browning) occurred mainly in areas covered by cropland gain (Fig. 7). This general information was consistent with the local degradation indicated out by the prevailing natural vegetation loss documented by the visual comparison of historical Google Earth images (Fig. S6). The comparison between the two sets of high spatial resolution images confirmed that the reduction and degradation of tiger bush (a typical banded vegetation pattern of trees and bushes, Fig. S6a) and general shrubs (Fig. S6b) were caused by high-intensity agricultural practices, such as overgrazing due to increased livestock increases (Hiernaux et al. 2009), wood cutting and clearing either for firewood and construction, or land clearing for crop fields (Abdi et al. 2014). In addition, agricultural practices, such as the use of slash-and-burn and mechanized methods to clear agricultural land (Fig. S6c), over-harvesting of wood for fuel and medicinal materials, and large-scale migration of grazing livestock to find more pastures not easily occupied by cropland expansion (Okore et al. 2007; Cotillon and Tappan 2016; Fiorillo et al. 2017; Tong et al. 2017; Biaou et al. 2021), have reduced the fractional abundance of natural vegetation in a short period. With the projected continuing population growth in Africa (Herrmann et al. 2020), more croplands are needed, which may lead to aggravating environmental degradation in the Sudano-Sahelian region. Therefore, more attention should be paid to the sustainable use of the land resources in this region.

Fire occurrence had large and significant negative effects on vegetation greenness in central West Africa. The majority of burned area occurred frequently in natural vegetation and cropland in central West Africa from 2001 to 2020 despite the fact that the total burned area decreased (Fig. S3a–c), resulting in a more significant NDVI reduction relative to unburned conditions (Fig. S3d). As mentioned above, fire is a traditional tool to increase agriculture production by converting natural vegetation areas to agricultural lands (slash-and-burn) and by managing pastures for livestock in African savannas, which inhibits tree growth and reduces the woody biomass (Singh et al. 2018). In addition, frequently repeated fires can reduce organic matter in the soil profile and reduce vegetation growth activity (Pellegrini et al. 2020, 2022). This means that fire occurrence is generally a serious threat to vegetation greenness over long periods of time (Wei et al. 2020; van Wees et al. 2021; Zhao et al. 2021b).

Limitations

There are several limitations of this study to consider. First, we did not evaluate the roles of other potential drivers, such as temperature, radiation, CO_2 concentration, grazing, and socio-economic conditions (Hiernaux et al. 2009; Lu et al. 2016; Devine et al. 2017; Piao et al. 2020; Abel et al. 2021), which have been reported as important drivers of global and local vegetation changes. Second, two statistical attribution models, i.e., the correlation-based conceptual attribution model and the relative importance approach, were used to assess the dominant drivers of NDVI trends. However, the models cannot reflect the direction of the impacts of the drivers, which may fail to directly reflect the positive or negative relationship between the drivers and the observed trends. For the regions where rainfall is the main limiting factor of vegetation growth, we also applied the Residual Trends (RESTREND) method

(Evans and Geerken 2004; Wessels et al. 2007; Leroux et al. 2017) in the areas with strong positive NDVI-rainfall correlations ($R \geq 0.5$) to test the importance of rainfall variability. The spatial pattern of residual NDVI trends was very close to that of NDVI trends (Fig. S7), and the NDVI residuals were too small and random to evaluate other relationships (Fig. S8). Therefore, we did not use the RESTREND method for attribution of NDVI trends to climatic and non-climatic factors. In fact, it is difficult to fully disentangle the impacts of climatic and non-climatic drivers on vegetation changes (Piao et al. 2020). The capacity and accuracy of the explanatory model of vegetation greenness change still requires other refined statistical attribution models coupled to integrated land surface/dynamic vegetation models.

Conclusions

This study contributed to a better understanding of the impacts of rainfall variability, LULC change, and fire occurrence change on vegetation greenness trends by using time-series satellite earth observation datasets in the Sudano-Sahelian region during 2001–2020. Our study documented a clear spatial heterogeneity in vegetation greenness trends; specifically, 26.9% of the region showed greening trends, whereas 5% of the region showed browning trends. Within the areas with greening trends, about half can be attributed to rainfall variability, i.e., rainfall-driven greening, which occurred mainly in the western Sahel, western Chad, and the Sudanian savannah. However, the dependence of browning on decreasing rainfall was not widespread. In addition to rainfall, the relative importance results suggested that LULC changes had substantial local effects on vegetation greenness and exhibited strong spatial heterogeneity in specific sub-regions, although the overall effect of LULC changes on vegetation greening or browning was relatively limited on average for the entire Sudano-Sahelian region. In Senegal and Ethiopia, cropland gain and natural vegetation gain related to positive land management were probably the dominant drivers of greening. The combined impacts of rainfall variability and LULC changes contributed to greening trends in the arid regions, especially in Mali and Sudan. In contrast, vegetation browning in central West Africa appeared to be driven by cropland expansion and natural vegetation loss associated with extensive agricultural production activities, which more attention should be paid to the sustainable natural resources management in this region in the context of continued population growth. In addition, we found that repeated fires for agricultural expansion in central West Africa intensified the browning of vegetation. The consideration of the combined factors related to rainfall, LULC, and fires is crucial to advance the current understanding of the potential drivers of vegetation greenness changes in the Sudano-Sahelian region.

Supplementary Information The online version contains supplementary material available at https://doi.org/10.1007/s10113-023-02084-5.

Acknowledgements The authors are thankful to the two anonymous reviewers for their critical comments and suggestions which were very helpful to improve the manuscript.

Funding This work was jointly supported by the projects funded by the Key Collaborative Research Program of the Alliance of International Science Organizations (Grant No. ANSO-CR-KP-2022–02), the Open Research Program of the International Research Center of Big Data for Sustainable Development Goals (Grant No. CBAS2023ORP05), the National Natural Science Foundation of China (NSFC) and United Nations Environmental Program (UNEP) (Grant No. 41661144022), the MOST High Level Foreign Expert program (Grant No. G2022055010L), and the Chinese Academy of Sciences President's International Fellowship Initiative (Grant No. 2020VTA0001).

Data availability The datasets analyzed during the current study are available from the corresponding author on request.

References

Abdi AM, Seaquist J, Tenenbaum DE, Eklundh L, Ardö J (2014) The supply and demand of net primary production in the Sahel. Environ Res Lett 9:11. https://doi.org/10.1088/1748-9326/9/9/094003

Abel C, Horion S, Tagesson T, De Keersmaecker W, Seddon AWR et al (2021) The human-environment nexus and vegetation-rainfall sensitivity in tropical drylands. Nature Sustainability 4:25–32. https://doi.org/10.1038/s41893-020-00597-z

Ahmed M, Else B, Eklundh L, Ardö J, Seaquist J (2017) Dynamic response of NDVI to soil moisture variations during different hydrological regimes in the Sahel region. Int J Remote Sens 38:5408–5429. https://doi.org/10.1080/01431161.2017.1339920

Ahmedou OCA, Nagasawa R, Osman AE, Hattori K (2008) Rainfall variability and vegetation dynamics in the Mauritanian Sahel. Climate Res 38:75–81. https://doi.org/10.3354/cr00776

Andela N, Morton DC, Giglio L, Chen Y, van der Werf GR et al (2017) A human-driven decline in global burned area. Science 356:1356–1362. https://doi.org/10.1126/science.aal4108

Andrieu J, Lombard F, Fall A, Thior M, Ba BD et al. (2020) Botanical field-study and remote sensing to describe mangrove resilience in the Saloum Delta (Senegal) after 30 years of degradation narrative. Forest Ecology and Management 461:117963. https://doi.org/10.1016/j.foreco.2020.117963

Archer SR, Andersen EM, Predick KI, Schwinning S, Steidl RJ et al (2017) Woody plant encroachment: causes and consequences. In: Briske DD (ed) Rangeland systems. Springer, Cham, pp 25–84. https://doi.org/10.1007/978-3-319-46709-2

Barnieh BA, Jia L, Menenti M, Zhou J, Zeng Y (2020) Mapping land use land cover transitions at different spatiotemporal scales in West Africa. Sustainability 12:8565. https://doi.org/10.3390/su12208565

Barnieh BA, Jia L, Menenti M, Jiang M, Zhou J et al (2022) Quantifying spatial reallocation of land use/land cover categories in West Africa. Ecol Indic 135:108556. https://doi.org/10.1016/j.ecolind.2022.108556

Bégué A, Vintrou E, Ruelland D, Claden M, Dessay N (2011) Can a 25-year trend in Soudano-Sahelian vegetation dynamics be interpreted in terms of land use change? A remote sensing approach. Glob Environ Chang 21:413–420. https://doi.org/10.1016/j.gloenvcha.2011.02.002

Berg A, Sheffield J (2018) Climate change and drought: the soil moisture perspective. Curr Clim Chang Rep 4:180–191. https://doi.org/10.1007/s40641-018-0095

Bergé Nguyen M, Crétaux JF (2015) Inundations in the Inner Niger Delta: monitoring and analysis using MODIS and global precipitation datasets. Remote Sens 7:2127–2151. https://doi.org/10.3390/rs70202127

Biaou S, Gouwakinnou GN, Biaou HSS, Tovihessi MS, Awessou BK et al (2021) Identifying the land use and land cover change drivers: methods and case studies of two forest reserves in Northern Benin. Environ Dev Sustain 24:1–21. https://doi.org/10.1007/s10668-021-01849-4

Bond WJ, Woodward FI, Midgley GF (2005) The global distribution of ecosystems in a world without fire. New Phytol 165:525–538. https://doi.org/10.1111/j.1469-8137.2004.01252.x

Borges J, Higginbottom TP, Cain B, Gadiye DE, Kisingo A et al (2022) Landsat time series reveal forest loss and woody encroachment in the Ngorongoro Conservation Area, Tanzania. Remote Sens Ecol Conserv 8:808–826. https://doi.org/10.1002/rse2.277

Boschetti M, Nutini F, Brivio PA, Bartholomé E, Stroppiana D et al (2013) Identification of environmental anomaly hot spots in West Africa from time series of NDVI and rainfall. ISPRS J Photogramm Remote Sens 78:26–40. https://doi.org/10.1016/j.isprsjprs.2013.01.003

Brandt M, Romankiewicz C, Spiekermann R, Samimi C (2014) Environmental change in time series - an interdisciplinary study in the Sahel of Mali and Senegal. J Arid Environ 105:52–63. https://doi.org/10.1016/j.jaridenv.2014.02.019

Brandt M, Rasmussen K, Hiernaux P, Herrmann S, Tucker CJ et al (2018) Reduction of tree cover in West African woodlands and promotion in semi-arid farmlands. Nat Geosci 11:328–333. https://doi.org/10.1038/s41561-018-0092-x

Brandt M, Hiernaux P, Rasmussen K, Tucker CJ, Wigneron J-P et al (2019) Changes in rainfall distribution promote woody foliage production in the Sahel. Commun Biol 2:133. https://doi.org/10.1038/s42003-019-0383-9

Camara BA, Sanogo D, Ndiaye O, Diahate PB, Sall M et al (2021) Farmers' perception on the benefits and constraints of Farmer Managed Natural Regeneration and determinants of its adoption in the southern groundnut basin of Senegal. Agrofor Syst 2021:1–14. https://doi.org/10.1007/s10457-021-00690-y

Camberlin P, Martiny N, Philippon N, Richard Y (2007) Determinants of the interannual relationships between remote sensed photosynthetic activity and rainfall in tropical Africa. Remote Sens Environ 106:199–216. https://doi.org/10.1016/j.rse.2006.08.009

Chen C, Park T, Wang X, Piao S, Xu B et al (2019) China and India lead in greening of the world through land-use management. Nat Sustain 2:122–129. https://doi.org/10.1038/s41893-019-0220-7

Cheng S, Huang J (2016) Enhanced soil moisture drying in transitional regions under a warming climate. J Geophys Res Atmos 121:2542–2555. https://doi.org/10.1002/2015JD024559

Cho J, Lee Y-W, Lee H-S (2015) The effect of precipitation and air temperature on land-cover change in the Sahel. Water Environ J 29:439–445. https://doi.org/10.1111/wej.12118

Cook KH, Vizy EK (2019) Contemporary climate change of the African monsoon systems. Curr Clim Chang Rep 5:145–159. https://doi.org/10.1007/s40641-019-00130-1

Cotillon SE, Tappan GG (2016) Landscapes of West Africa: a window on a changing world. United States Geological Survey, Garretson, SD, USA. https://doi.org/10.5066/F7N014QZ

D'Adamo F, Ogutu B, Brandt M, Schurgers G, Dash J (2021) Climatic and non-climatic vegetation cover changes in the rangelands of Africa. Global Planet Chang 202:103516. https://doi.org/10.1016/j.gloplacha.2021.103516

Dardel C, Kergoat L, Hiernaux P, Mougin E, Grippa M et al (2014a) Re-greening Sahel: 30 years of remote sensing data and field observations (Mali, Niger). Remote Sens Environ 140:350–364. https://doi.org/10.1016/j.rse.2013.09.011

Dardel C, Kergoat L, Hiernaux P, Grippa M, Mougin E et al (2014b) Rain-use-efficiency: what it tells us about the conflicting Sahel greening and Sahelian paradox. Remote Sens 6:3446–3474. https://doi.org/10.3390/rs6043446

Dembélé M, Zwart SJ (2016) Evaluation and comparison of satellite-based rainfall products in Burkina Faso, West Africa. Int J Remote Sens 37:3995–4014. https://doi.org/10.1080/01431161.2016.1207258

Devine AP, McDonald RA, Quaife T, Maclean IM (2017) Determinants of woody encroachment and cover in African savannas. Oecologia 183:939–951. https://doi.org/10.1007/s00442-017-3807-6

Endris HS, Lennard C, Hewitson B, Dosio A, Nikulin G et al (2019) Future changes in rainfall associated with ENSO, IOD and changes in the mean state over Eastern Africa. Clim Dyn 52:2029–2053. https://doi.org/10.1007/s00382-018-4239-7

Evans J, Geerken R (2004) Discrimination between climate and human-induced dryland degradation. J Arid Environ 57:535–554. https://doi.org/10.1016/S0140-1963(03)00121-6

Fensholt R, Mbow C, Brandt M, Rasmussen K (2017) Desertification and re-greening of the Sahel. Oxford Research Encyclopedia of Climate Science, Oxford University. https://doi.org/10.1093/acrefore/9780190228620.013.553

Fensholt R, Rasmussen K (2011) Analysis of trends in the Sahelian 'rain-use efficiency' using GIMMS NDVI, RFE and GPCP rainfall data. Remote Sens Environ 115:438–451. https://doi.org/10.1016/j.rse.2010.09.014

Fent A, Bardou R, Carney J, Cavanaugh K (2019) Transborder political ecology of mangroves in Senegal and The Gambia. Glob Environ Chang 54:214–226. https://doi.org/10.1016/j.gloenvcha.2019.01.003

Fiorillo E, Maselli F, Tarchiani V, Vignaroli P (2017) Analysis of land degradation processes on a tiger bush plateau in South West Niger using MODIS and LANDSAT TM/ETM+ data. Int J Appl Earth Obs Geoinf 62:56–68. https://doi.org/10.1016/j.jag.2017.05.010

Foley JA, Ramankutty N, Brauman KA, Cassidy ES, Gerber JS et al (2011) Solutions for a cultivated planet. Nature 478:337–342. https://doi.org/10.1038/nature10452

Fu B, Stafford-Smith M, Wang Y, Wu B, Yu X et al (2021) The Global-DEP conceptual framework—research on dryland ecosystems to promote sustainability. Curr Opin Environ Sustain 48:17–28. https://doi.org/10.1016/j.cosust.2020.08.009

Funk C, Peterson P, Landsfeld M, Pedreros D, Verdin J et al (2015) The climate hazards infrared precipitation with stations-a new environmental record for monitoring extremes. Sci Data 2:150066. https://doi.org/10.1038/sdata.2015.66

Gashaw T (2015) The implications of watershed management for reversing land degradation in Ethiopia. Res J Agric Environ Manag 4:5–12. https://www.apexjournal.org/rjaem/archive/2015/Jan/abstract/Gashaw.htm

Giannini A, Biasutti M, Verstraete MM (2008) A climate model-based review of drought in the Sahel: desertification, the re-greening and climate change. Global Planet Change 64:119–128. https://doi.org/10.1016/j.gloplacha.2008.05.004

Gong P, Li X, Wang J, Bai Y, Chen B et al (2020) Annual maps of global artificial impervious area (GAIA) between 1985 and 2018. Remote Sens Environ 236:111510. https://doi.org/10.1016/j.rse.2019.111510

Gorsevski V, Kasischke E, Dempewolf J, Loboda T, Grossmann F (2012) Analysis of the Impacts of armed conflict on the Eastern Afromontane forest region on the South Sudan - Uganda border using multitemporal Landsat imagery. Remote Sens Environ 118:10–20. https://doi.org/10.1016/j.rse.2011.10.023

Grömping U (2006) Relative importance for linear regression in R: The package relaimpo. J Stat Softw 17:1–27. https://doi.org/10.18637/jss.v017.i01

Hansen MC, Potapov PV, Moore R, Hancher M, Turubanova SA et al (2013) High-resolution global maps of 21st-century forest cover change. Science 342:850–853. https://doi.org/10.1126/science.1244693

Haregeweyn N, Berhe A, Tsunekawa A, Tsubo M, Meshesha DT (2012) Integrated watershed management as an effective approach to curb land degradation: a case study of the Enabered Watershed in northern Ethiopia. Environ Manage 50:1219–1233. https://doi.org/10.1007/s00267-012-9952-0

Helldén U, Tottrup C (2008) Regional desertification: a global synthesis. Global Planet Change 64:169–176. https://doi.org/10.1016/j.gloplacha.2008.10.006

Herrmann SM, Anyamba A, Tucker CJ (2005) Recent trends in vegetation dynamics in the African Sahel and their relationship to climate. Glob Environ Chang 15:394–404. https://doi.org/10.1016/j.gloenvcha.2005.08.004

Herrmann SM, Brandt M, Rasmussen K, Fensholt R (2020) Accelerating land cover change in West Africa over four decades as population pressure increased. Commun Earth Environ 1:53. https://doi.org/10.1038/s43247-020-00053-y

Hickler T, Eklundh L, Seaquist JW, Smith B, Ardö J et al (2005) Precipitation controls Sahel greening trend. Geophys Res Lett 32:L21415. https://doi.org/10.1029/2005GL024370

Hiernaux P, Ayantunde A, Kalilou A, Mougin E, Gerard B et al (2009) Trends in productivity of crops, fallow and rangelands in Southwest Niger: impact of land use, management and variable rainfall. J Hydrol 375:65–77. https://doi.org/10.1016/j.jhydrol.2009.01.032

Hoscilo A, Balzter H, Bartholomé E, Boschetti M, Brivio PA et al (2015) A conceptual model for assessing rainfall and vegetation trends in sub-Saharan Africa from satellite data. Int J Climatol 35:3582–3592. https://doi.org/10.1002/joc.4231

Hu Q, Xiang M, Chen D, Zhou J, Wu W et al (2020) Global cropland intensification surpassed expansion between 2000 and 2010: a spatio-temporal analysis based on GlobeLand30. Sci Total Environ 746:141035. https://doi.org/10.1016/j.scitotenv.2020.141035

Huber S, Fensholt R, Rasmussen K (2011) Water availability as the driver of vegetation dynamics in the African Sahel from 1982 to 2007. Global Planet Change 76:186–195. https://doi.org/10.1016/j.gloplacha.2011.01.006

Jiang M, Jia L, Menenti M, Zeng Y (2022) Understanding spatial patterns in the drivers of greenness trends in the Sahel-Sudano-Guinean region. Big Earth Data 2022:1–20. https://doi.org/10.1080/20964471.2022.2146632

Jin J, Yan T, Zhu Q, Wang Y, Guo F et al (2021) Heterogeneity of land cover data with discrete classes obscured remotely-sensed detection of sensitivity of forest photosynthesis to climate. Int J Appl Earth Obs Geoinformation 104:102567. https://doi.org/10.1016/j.jag.2021.102567

Kaptué AT, Prihodko L, Hanan NP (2015) On regreening and degradation in Sahelian watersheds. Proc Natl Acad Sci USA 112:12133–12138. https://doi.org/10.1073/pnas.1509645112

Kelly BA, Sanogo S, Sidibé SI, Castillo-Lorenzo E, Ceci P et al (2021) Restoring vegetation and degraded lands by using assisted natural regeneration approach (ANRA): case study at Bankass in the centre of Mali, West Africa. Environ Dev Sustain 23:14123–14139. https://doi.org/10.1007/s10668-021-01223-4

Kusserow H (2017) Desertification, resilience, and re-greening in the African Sahel - a matter of the observation period? Earth Syst Dyn 8:1141–1170. https://doi.org/10.5194/esd-8-1141-2017

Le Houérou HN (1984) Rain use efficiency: a unifying concept in arid-land ecology. J Arid Environ 7:213–247. https://doi.org/10.1016/S0140-1963(18)31362-4

Lebel T, Cappelaere B, Galle S, Hanan N, Kergoat L et al (2009) AMMA-CATCH studies in the Sahelian region of West-Africa: An overview. J Hydrol 375:3–13. https://doi.org/10.1016/j.jhydrol.2009.03.020

Leroux L, Bégué A, Lo Seen D, Jolivot A, Kayitakire F (2017) Driving forces of recent vegetation changes in the Sahel: lessons learned from regional and local level analyses. Remote Sens Environ 191:38–54. https://doi.org/10.1016/j.rse.2017.01.014

Leroux L, Bégué A, Lo Seen D (2014) Regional analysis of crop and natural vegetation in West Africa based on NDVI metrics. IEEE Geoscience and Remote Sensing Symposium pp. 5107–5110. https://doi.org/10.1109/IGARSS.2014.6947646

Li C, Gong P, Wang J, Zhu Z, Biging GS et al (2017) The first all-season sample set for mapping global land cover with Landsat-8 data. Science Bulletin 62:508–515. https://doi.org/10.1016/j.scib.2017.03.011

Li W, Du J, Li S, Zhou X, Duan Z et al (2019) The variation of vegetation productivity and its relationship to temperature and precipitation based on the GLASS-LAI of different African ecosystems from 1982 to 2013. Int J Biometeorol 63:847–860. https://doi.org/10.1007/s00484-019-01698-x

Lindeman RH, Merenda PF, Gold RZ (1980) Introduction to bivariate and multivariate analysis. Scott, Foresman, Glenview, Illinois

Lizundia-Loiola J, Otón G, Ramo R, Chuvieco E (2020) A spatio-temporal active-fire clustering approach for global burned area mapping at 250 m from MODIS data. Remote Sens Environ 236:111493. https://doi.org/10.1016/j.rse.2019.111493

Lu X, Wang L, McCabe MF (2016) Elevated CO2 as a driver of global dryland greening. Sci Rep 6:20716. https://doi.org/10.1038/srep20716

Martiny N, Richard Y, Camberlin P (2005) Interannual persistence effects in vegetation dynamics of semi-arid Africa. Geophys Res Lett 32:L24403. https://doi.org/10.1029/2005GL024634

Masiliūnas D, Tsendbazar N-E, Herold M, Lesiv M, Buchhorn M et al (2021) Global land characterisation using land cover fractions at 100 m resolution. Remote Sens Environ 259:112409. https://doi.org/10.1016/j.rse.2021.112409

Menenti M, Azzali S, Verhoef W, Vanswol R (1993) Mapping agro-ecological zones and time lag in vegetation growth by means of fourier analysis of time series of NDVI images. Adv Space Res 13:233–237. https://doi.org/10.1016/0273-1177(93)90550-U

Milas S (1984) Population crisis and desertification in the Sudano-Sahelian Region. Environ Conserv 11:167–169. https://doi.org/10.1017/S0376892900013850

Mills AJ, Milewski AV, Fey MV, Gröngröft A, Petersen A et al (2013) Constraint on woody cover in relation to nutrient content of soils in western southern Africa. Oikos 122:136–148. https://doi.org/10.1111/j.1600-0706.2012.20417.x

Mood AM (1950) Introduction to the theory of statistics. MacGraw-Hill, New York

Nicholson SE (2009) A revised picture of the structure of the "monsoon" and land ITCZ over West Africa. Clim Dyn 32:1155–1171. https://doi.org/10.1007/s00382-008-0514-3

Nicholson SE (2013) The West African Sahel: a review of recent studies on the rainfall regime and its interannual variability. Int Scholarly Res Not 2013:1–32. https://doi.org/10.1155/2013/453521

Nicholson SE (2017) Climate and climatic variability of rainfall over eastern Africa. Rev Geophys 55:590–635. https://doi.org/10.1002/2016RG000544

Noy-Meir I (1973) Desert ecosystems: environment and producers. Annu Rev Ecol Syst 4:25–51. https://doi.org/10.1146/annurev.es.04.110173.000325

Nutini F, Boschetti M, Brivio PA, Bocchi S, Antoninetti M (2013) Land-use and land-cover change detection in a semi-arid area of Niger using multi-temporal analysis of Landsat images. Int J Remote Sens 34:4769–4790. https://doi.org/10.1080/01431161.2013.781702

Oates N, Hisberg A, Ros JR, Solomon H, Ludi E et al (2020) The implications of state intervention for self-governed irrigation schemes: insights from Tigray, Ethiopia. Irrig Drain 69:88–99. https://doi.org/10.1002/ird.2121

Ogilvie A, Poussin J-C, Bader J-C, Bayo F, Bodian A et al (2020) Combining multi-sensor satellite imagery to improve long-term monitoring of temporary surface water bodies in the Senegal River Floodplain. Remote Sens 12:3157. https://doi.org/10.3390/rs12193157

Ogutu BO, D'Adamo F, Dash J (2021) Impact of vegetation greening on carbon and water cycle in the African Sahel-Sudano-Guinean region. Global Planet Chang 202:103524. https://doi.org/10.1016/j.gloplacha.2021.103524

Okore IK, Tijani-Eniola H, Agboola AA, Aiyelari EA (2007) Impact of land clearing methods and cropping systems on labile soil C and N pools in the humid zone Forest of Nigeria. Agr Ecosyst Environ 120:250–258. https://doi.org/10.1016/j.agee.2006.09.011

Olsson L, Eklundh L, Ardö J (2005) A recent greening of the Sahel—trends, patterns and potential causes. J Arid Environ 63:556–566. https://doi.org/10.1016/j.jaridenv.2005.03.008

Pasiecznik N, Reij C (2020) Restoring African Drylands. Tropenbos International, Wageningen, the Netherlands. http://www.etfrn.org/publications/restoring+african+drylands

Pausas JG, Ribeiro E (2013) The global fire–productivity relationship. Glob Ecol Biogeogr 22:728–736. https://doi.org/10.1111/geb.12043

Pekel J-F, Cottam A, Gorelick N, Belward AS (2016) High-resolution mapping of global surface water and its long-term changes. Nature 540:418–422. https://doi.org/10.1038/nature20584

Pellegrini AF, Hobbie SE, Reich PB, Jumpponen A, Brookshire EJ et al (2020) Repeated fire shifts carbon and nitrogen cycling by changing plant inputs and soil decomposition across ecosystems. Ecological Monographs 90:e01409. https://doi.org/10.1002/ecm.1409

Pellegrini AF, Harden J, Georgiou K, Hemes KS, Malhotra A et al (2022) Fire effects on the persistence of soil organic matter and long-term carbon storage. Nat Geosci 15:5–13. https://doi.org/10.1038/s41561-021-00867-1

Piao S, Wang X, Park T, Chen C, Lian X et al (2020) Characteristics, drivers and feedbacks of global greening. Nat Rev Earth Environ 1:14–27. https://doi.org/10.1038/s43017-019-0001-x

Ramel R, Gallee H, Messager C (2006) On the northward shift of the West African monsoon. Clim Dyn 26:429–440. https://doi.org/10.1007/s00382-005-0093-5

Ramo R, Roteta E, Bistinas I, van Wees D, Bastarrika A et al (2021) African burned area and fire carbon emissions are strongly impacted by small fires undetected by coarse resolution satellite data. Proc Natl Acad Sci USA 118:e2011160118. https://doi.org/10.1073/pnas.2011160118

Rasmussen K, Fensholt R, Fog B, Vang Rasmussen L, Yanogo I (2014) Explaining NDVI trends in northern Burkina Faso. Geogr Tidsskr 114:17–24. https://doi.org/10.1080/00167223.2014.890522

Reij C, Tappan G, Smale M (2009) Agroenvironmental transformation in the Sahel: another kind of "Green Revolution". International Food Policy Research Institute, Washington, DC. http://www.ifpri.org/publication/agroenvironmental-transformation-sahel

Rigge M, Shi H, Homer C, Danielson P, Granneman B (2019) Long-term trajectories of fractional component change in the Northern Great Basin, USA. Ecosphere 10:e02762. https://doi.org/10.1002/ecs2.2762

Rishmawi K, Prince SD (2016) Environmental and anthropogenic degradation of vegetation in the Sahel from 1982 to 2006. Remote Sens 8:948. https://doi.org/10.3390/rs8110948

Ruelland D, Levavasseur F, Tribotté A (2010) Patterns and dynamics of land-cover changes since the 1960s over three experimental areas in Mali. Int J Appl Earth Obs Geoinf 12:S11–S17. https://doi.org/10.1016/j.jag.2009.10.006

Shono K, Cadaweng EA, Durst PB (2007) Application of assisted natural regeneration to restore degraded tropical forestlands. Restor Ecol 15:620–626. https://doi.org/10.1111/j.1526-100X.2007.00274.x

Singh J, Levick SR, Guderle M, Schmullius C, Trumbore SE (2018) Variability in fire-induced change to vegetation physiognomy and biomass in semi-arid savanna. Ecosphere 9:e02514. https://doi.org/10.1002/ecs2.2514

Song X-P, Hansen MC, Stehman SV, Potapov PV, Tyukavina A et al (2018) Global land change from 1982 to 2016. Nature 560:639–643. https://doi.org/10.1038/s41586-018-0411-9

Staver AC (2018) Prediction and scale in savanna ecosystems. New Phytol 219:52–57. https://doi.org/10.1111/nph.14829

Stevens N, Bond W, Feurdean A, Lehmann CE (2022) Grassy ecosystems in the Anthropocene. Annu Rev Environ Resour 47:261–289. https://doi.org/10.1146/annurev-environ-112420-015211

Tadele Z (2017) Raising crop productivity in Africa through intensification. Agronomy 7:22. https://doi.org/10.3390/agronomy7010022

Tappan GG, Sall M, Wood EC, Cushing M (2004) Ecoregions and land cover trends in Senegal. J Arid Environ 59:427–462. https://doi.org/10.1016/j.jaridenv.2004.03.018

Teka K, Haftu M, Ostwald M, Cederberg C (2020) Can integrated watershed management reduce soil erosion and improve livelihoods? A study from northern Ethiopia. Int Soil Water Conserv Res 8:266–276. https://doi.org/10.1016/j.iswcr.2020.06.007

Tian F, Brandt M, Liu YY, Verger A, Tagesson T et al (2016) Remote sensing of vegetation dynamics in drylands: Evaluating vegetation optical depth (VOD) using AVHRR NDVI and in situ green biomass data over West African Sahel. Remote Sens Environ 177:265–276. https://doi.org/10.1016/j.rse.2016.02.056

Tong X, Brandt M, Hiernaux P, Herrmann SM, Tian F et al (2017) Revisiting the coupling between NDVI trends and cropland changes in the Sahel drylands: a case study in western Niger. Remote Sens Environ 191:286–296. https://doi.org/10.1016/j.rse.2017.01.030

Toté C, Patricio D, Boogaard H, Van der Wijngaart R, Tarnavsky E et al (2015) Evaluation of satellite rainfall estimates for drought and flood monitoring in Mozambique. Remote Sens 7:1758–1776. https://doi.org/10.3390/rs70201758

Trabucco A, Zomer RJ (2018) Global aridity index and potential evapotranspiration (ET0) climate database v2. CGIAR-Consortium for Spatial Information. 10.6084/m9.figshare.7504448.v2

van Wees D, van der Werf GR, Randerson JT, Andela N, Chen Y et al (2021) The role of fire in global forest loss dynamics. Glob Change Biol 27:2377–2391. https://doi.org/10.1111/gcb.15591

Venter ZS, Cramer MD, Hawkins HJ (2018) Drivers of woody plant encroachment over Africa. Nat Commun 9:2272. https://doi.org/10.1038/s41467-018-04616-8

Wang'ati FJ (1996) The impact of climate variation and sustainable development in the Sudano-Sahelian region. In: Ribot JC, Magalhaes AM, Panagides SS (eds) Climate variability, climate change and social vulnerability in the Semi-Arid Tropics. Cambridge University Press, pp 71–91. https://doi.org/10.1017/CBO9780511608308.006

Wei F, Wang S, Fu B, Brandt M, Pan N et al (2020) Nonlinear dynamics of fires in Africa over recent decades controlled by precipitation. Glob Change Biol 26:4495–4505. https://doi.org/10.1111/gcb.15190

Wei F, Wang S, Brandt M, Fu B, Meadows ME et al (2021) Responses and feedbacks of African dryland ecosystems to environmental changes. Curr Opin Environ Sustain 48:29–35. https://doi.org/10.1016/j.cosust.2020.09.004

Wessels KJ, Prince SD, Malherbe J, Small J, Frost PE et al (2007) Can human-induced land degradation be distinguished from the effects of rainfall variability? A case study in South Africa. J Arid Environ 68:271–297. https://doi.org/10.1016/j.jaridenv.2006.05.015

Wortmann CS, Stewart Z (2021) Nutrient management for sustainable food crop intensification in African tropical savannas. Agron J 113:4605–4615. https://doi.org/10.1002/agj2.20851

Xu Y, Yu L, Zhao FR, Cai X, Zhao J et al (2018) Tracking annual cropland changes from 1984 to 2016 using time-series Landsat images with a change-detection and post-classification approach: Experiments from three sites in Africa. Remote Sens Environ 218:13–31. https://doi.org/10.1016/j.rse.2018.09.008

Yu L (2022) 30m land use and cover maps for the Sahel-Sudano-Guinean region of Africa (1990–2020). National Tibetan Plateau/Third Pole Environment Data Center. https://doi.org/10.11888/Terre.tpdc.272021

Yue S, Pilon P, Phinney B, Cavadias G (2002) The influence of autocorrelation on the ability to detect trend in hydrological series. Hydrol Process 16:1807–1829. https://doi.org/10.1002/hyp.1095

Zhang W, Brandt M, Tong X, Tian Q, Fensholt R (2018) Impacts of the seasonal distribution of rainfall on vegetation productivity across the Sahel. Biogeosciences 15:319–330. https://doi.org/10.5194/bg-15-319-2018

Zhang W, Brandt M, Penuelas J, Guichard F, Tong X et al (2019) Ecosystem structural changes controlled by altered rainfall climatology in tropical savannas. Nat Commun 10:671. https://doi.org/10.1038/s41467-019-08602-6

Zhao J, Yu L, Liu H, Huang H, Wang J et al (2021a) Towards an open and synergistic framework for mapping global land cover. Peerj 9:e11877. https://doi.org/10.7717/peerj.11877

Zhao Z, Li W, Ciais P, Santoro M, Cartus O et al (2021b) Fire enhances forest degradation within forest edge zones in Africa. Nat Geosci 14:479–483. https://doi.org/10.1038/s41561-021-00763-8

Zhou J, Jia L, Menenti M, van Hoek M, Lu J et al (2021a) Characterizing vegetation response to rainfall at multiple temporal scales in the Sahel-Sudano-Guinean region using transfer function analysis. Remote Sens Environ 252:112108. https://doi.org/10.1016/j.rse.2020.112108

Zhou J, Jia L, Menenti M, Liu X (2021b) Optimal estimate of global biome-specific parameter settings to reconstruct NDVI time series with the harmonic analysis of time series (HANTS) method. Remote Sens 13:4251. https://doi.org/10.3390/rs13214251

Zhou J, Jia L, van Hoek M, Menenti M, Lu J et al (2016) An optimization of parameter settings in HANTS for global NDVI time series reconstruction. 2016 IEEE International Geoscience and Remote Sensing Symposium (IGARRS) pp. 3422–3425. https://doi.org/10.1109/Igarss.2016.7729884

Zhu Z, Piao S, Myneni RB, Huang M, Zeng Z et al (2016) Greening of the Earth and its drivers. Nat Clim Chang 6:791–795. https://doi.org/10.1038/nclimate3004

Zhu Z, Qiu S, Ye S (2022) Remote sensing of land change: a multifaceted perspective. Remote Sens Environ 282:113266. https://doi.org/10.1016/j.rse.2022.113266

Zoungrana BJ-B, Conrad C, Thiel M, Amekudzi LK, Da ED (2018) MODIS NDVI trends and fractional land cover change for improved assessments of vegetation degradation in Burkina Faso, West Africa. J Arid Environ 153:66–75. https://doi.org/10.1016/j.jaridenv.2018.01.005

Zubkova M, Boschetti L, Abatzoglou JT, Giglio L (2019) Changes in fire activity in Africa from 2002 to 2016 and their potential drivers. Geophys Res Lett 46:7643–7653. https://doi.org/10.1029/2019GL083469